Università degli Studi di Padova

Head Office: Università degli Studi di Padova

Department

Molecular Medicine

Ph.D. COURSE IN: Molecular Medicine

CURRICULUM: Regenerative Medicine

SERIES XXXII Cycle

EXPLORING THE DIMORPHISM DURING FIBROSIS DEVELOPMENT AND REGRESSION IN A MURINE MODEL OF TOXIN-INDUCED CHRONIC LIVER INJURY

Coordinator: Prof. Stefano Piccolo

Supervisor: Prof. Francesco Paolo Russo

Ph.D. Candidate: Dr. Marika Crescenzi

Index

List of Abbreviations

AIH Autoimmune hepatitis
α-SMA Alpha smooth muscle actin
BM Bone marrow
CCl_4 Carbon tetrachloride
CK-7 Cytokeratin-7
CLD Chronic liver disease
DRs Ductular reactions
DT diphtheria toxin
DTR diphtheria toxin receptor
ECM Extra-cellular matrix
EMT Epithelial mesenchymal transition
FAH fumarylacetoacetate hydrolase
FCM Flow Cytometry
GATA6 GATA-binding factor 6
GFAP Glial fibrillary acidic protein
HCC Hepatocellular carcinoma
HCV Hepatitis C Virus
hbEGF heparin-binding Epithelial Growth Factor
H&E Hematoxylin and Eosin
HSCs Hepatic stellate cells
IHC Immunohistochemistry
IFN-γ Interferon gamma
IL-1 Interleukin-1
IL-6 Interleukin-6
IRI Ischemia and reperfusion injury
KCs Kupffer cells
LF Liver fibrosis
LOD Limit of detection
LPCs Liver progenitor cells
LSEC Liver sinusoidal endothelial cells
MDMs Monocyte-derived macrophages
MMPs Metalloproteinases

MSCs Mesenchymal stem cells

NASH Non-alcoholic steatohepatitis

NK Natural killer

PH Partial hepatectomy

PSC Primary Sclerosing Cholangitis

SAMs Scar associated macrophages

TGF-β Transforming growth factor beta

TIMPs Tissue inhibitors of metalloproteinases

TNF-α Tumor necrosis factor alpha

TWEAK TNF-related weak inducer of apoptosis

WT Wild type

Summary

Liver fibrosis represents a crucial biological process, being the final common pathway of chronic or iterative liver damage. It is consequent to repeated wounds which are known to heal not in a timely manner. The contribution of gender-biased hepatic responses to liver injury represents a lively research topic to be investigated. With this PhD research the crosstalk between fibrosis, the drivers and targets of matrix remodelling and the hepatic immune microenvironment was ascertained and characterized. A murine model of chronic hepatic damage established by repeated administrations of the toxin CCl_4 was developed and the injured liver was analysed in a timeframe of 12 weeks, including in addition also a period of washout of 8 weeks which allowed the liver to self-heal. Fibrosis, HSCs activation, analysis of matrix remodelling players in the liver along with immune infiltrating cellular components and circulating sexual hormones and cytokines were deeply investigated. An impaired capability for injured females to resorb excessive hepatic ECM during the self-healing was demonstrated, associated both with a decrease in estradiol concentrations and a delayed MMP9 activity in the onset of chronic hepatic damage. The characterization of the fibrotic milieu demonstrated an imbalance in the axis MMP-TIMP associated with a more inflammatory prone immune profile in female mice. The differences in the immune profile between injured males and females were also confirmed by analysing an array of circulating cytokines. The investigations in liver single cell suspensions of the immune cellular components present accordingly to different stages of severity of the disease, unveiled a residual population of Kupffer cells in females and a restorative macrophages component in males, after the self-healing, which could be responsible for the gender-biased effective fibrosis resolution. Further investigations are needed to ascertain if an angiocrine altered signalling is also part of this imbalance, considering data obtained on VEGFA mRNAs and protein modulations. Moreover, the possibility to translate into other models of hepatic injury data evidenced by this PhD thesis and, above all, to study in humans the biological processes below the liver dimorphism in fibrosis dynamics represents a mandatory condition to augment the knowledge in this lively field of research.

Introduction

Liver as a dimorphic organ

The liver is highly dimorphic and a gender disparity is observed in various types of liver injury, including autoimmune hepatitis, cholestatic disorders, non-alcoholic fatty liver disease, and during hepatic carcinogenesis. Sex hormones might modulate hepatic inflammation by regulating the function of the immune system [Schwinge *et al*., 2015]. The mechanisms of sex differences in inflammatory and immune responses in the liver are not yet fully elucidated. For example, in a mouse model of Concanavalin A-mediated acute hepatitis, standard operating procedures recommend to use only male animals due to the more pronounced and reproducible induction of the hepatic immune activation [Heymann *et al*., 2015]. The presence of sexual dimorphism was also reported in cutaneous wound-healing [Gilliver *et al*., 2008], suggesting that regenerative and scarring responses are influenced by gender.

Hepatic Immune system

The innate immune system in the liver is comprised of the liver resident KCs, dendritic cells, NK cells, and NKT cells [Bilzer *at al*., 2006; Santodomingo-Garzon *et al*., 2011; Seki *et al*., 2011; Guicciardi *et al*., 2013]. Moreover, innate immune functions are also ascribed to hepatocytes, LSEC, HSC, and cholangiocytes [Fava *et al*., 2005; Winau *et al*., 2007]. Besides the surveillance functions of the intestinal innate immune system, the liver is the second line of defence toward different gut-derived endobiotics, xenobiotics, and bacterial products [Gao *et al*., 2008]. This has led to the evolution of a very particular innate immune system in the liver, characterized by tolerance toward a vast array of non self and self-antigens [Tiegs *et al*., 2010] which permits concurrent solid organ transplantation and transplantation across MHC barriers. Unfortunately, it is due to the permissive immune tolerant state of the liver which the establishment of chronic viral hepatitis is allowed [Protzer *et al*., 2012]. Another feature of non-microbial acute and chronic liver diseases is activation of the innate immune system, defined sterile inflammation [Chen *et al*., 2010] Though the innate immune system facilitates both inflammation and tissue healing in acute hepatitis, in chronic liver diseases, its chronic activation likely forms the basis for chronic inflammation.

How chronic wound healing affects hepatic microenvironment

The healthy liver is rich in a plethora of cytokines (e.g., IL-1α, IL-1β, TNFα, and IL-6) and growth factors (e.g., IGF, EGF and TGF-α) that stimulate hepatocyte growth and induce activation upon the correct stimuli [Ramadori *et al*., 2001; Fernandez *et al*., 2019]. Following tissue injury, KCs, liver-specific macrophages, secrete pro-inflammatory cytokines such as IL-1, IL-6, and TNF-α [Tsutsui *et*

al., 2014]. TNF-α plays a key role in maintaining liver homeostasis by promoting tissue regeneration along with IL-6 in an STAT3/NFκB-dependent manner [Sudo *et al*., 2008]. If the wound is repaired, KCs shift their phenotype secreting anti-inflammatory cytokines such as IL-4 or IL-10 [Knolle *et al*., 1995]. In particular, IL-10 is a potent anti-inflammatory cytokine which suppresses monocyte infiltration and counteracts synthesis of both proinflammatory mediators and collagen by myofibroblasts [Tilg *et al*., 2006]. In a clinical trial with IL-10 in patients with chronic hepatitis C a reduction in fibrosis and improvements in liver histology and function are reported [Nelson *et al*., 2000].

Uninterrupted liver injury and chronic liver disease determine a state of perpetual inflammation that can support malignant transformation [Bishayee *et al*., 2014]. Pro-inflammatory cytokine levels are particularly high at early stages of tumor development, indicating that during tumor formation, a pro-inflammatory environment plays a role in tumor development [Ueda *et al*., 1994]. While the cytokines and growth factors associated with inflammation may support tumor growth at these early stages, they also activate cytotoxic immune cells, strengthening a cycle of immune-mediated tumor cell death and birth. The term "immunoediting" is often used to describe an evolutionary process on tumor development driven by the immune system [Mittal *et al.*, 2014]

The fine orchestration of cells and soluble factors, not only the expression or extinction of certain critical mediator but also their tuning and timing during inflammation determines the resolution of inflammation. However, under certain circumstances the inflammatory stimuli persist and the regulatory mechanism runs out of control (prolonged or excessive response, inadequate production of resolution mediators), the non resolving inflammation occurs and may have pathological consequences, such as fibrosis or tumor growth [Medzhitov 2008¸Yu *et al*., 2018] (Figure 1).

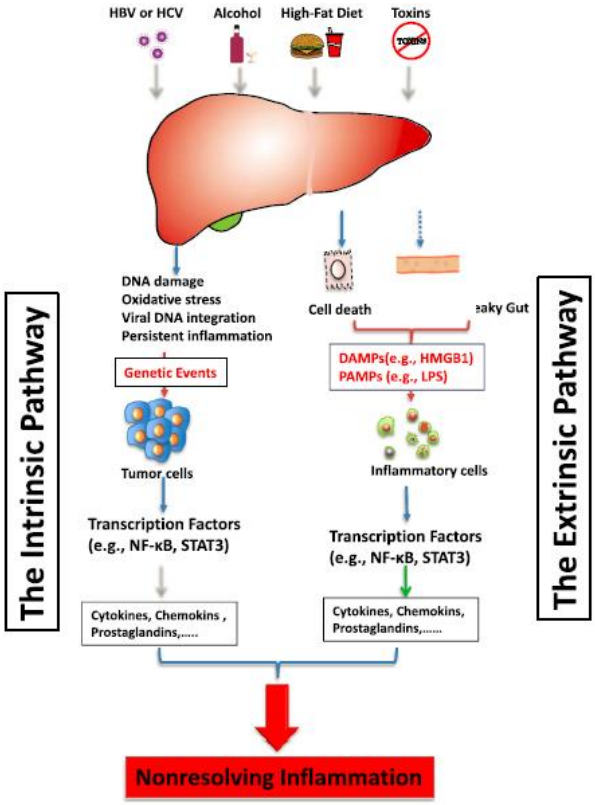

Figure 1. The extrinsic and intrinsic pathways that trigger non resolving inflammation. The extrinsic pathway is driven by exogenous factors (e.g., the PAMPs from pathogens or DAMPs from dead cells), which trigger a persistent inflammatory response by engaging the receptors expressed in the inflammatory cells and establish an inflammatory condition that increase cancer risk. The intrinsic pathway is induced by alterations in cancer-associated genetic factors (e.g., mutation of either oncogenes or tumor suppressor genes), which activate the expression of inflammation-related program. Both of these pathways activate transcription factors (e.g., NF-κB, STAT3) that coordinate the production of inflammatory mediators, ROS, NOS, etc. creating a pro-tumor inflammatory microenvironment in the liver [in Yu *et al*., 2018].

Generally, chronic wound healing implies a highly complex and dynamic interplay between injured parenchymal cells, myofibroblasts, inflammatory cells, and tissue-specific stem and progenitor cells [Forbes *et al*., 2016]. The liver houses a specialised macrophage population known as Kupffer cells. Following injury, the liver's macrophage population changes and it also dramatically expands through monocyte recruitment from circulation. Monocytes differentiate into monocyte-derived macrophages (MDMs) upon infiltration into the damaged organ [Karlmark *et al*., 2009]. Data from literature demonstrate that KCs are key maintainers of liver homeostasis and early responders to liver injury [Kolios, *et al*., 2006]. On the other hand, MDMs are crucial for inflammation and tissue repair following liver injury [Tacke *et al*., 2014]. In fact, during liver repair, the number of KCs decreases with a substantial increase in the number of MDMs [Holt *et al*., 2008].

Duffield and co-workers, in an elegant study published in 2005, using the CD11b-DTR transgenic mouse, established that macrophage depletion during liver injury-inflammation prevents the development of liver fibrosis. Conversely, depletion during recovery attenuates the degradation of matrix proteins [Duffield *et al*., 2005]. These divergent roles remind us the plasticity of macrophages. This cell population adapts its phenotype in response to signals from the microenvironment. To oversimplify the heterogeneity of macrophage phenotypes, two main phenotypes are recognized for macrophages, classified as M1 (classically activated) or M2 (alternatively activated) [Stout *et al*., 2004]. M1 macrophages are recognized as pro-inflammatory, releasing cytokines such as TNFα, IL-1β, and IL-6 [Mantovani *et al*., 2005]. M2 macrophages are associated with immunomodulation and tissue repair and display an important capacity for phagocytosis and factors release (IL-10, TGFβ, and MMPs) [Shapouri-Moghaddam *et al*., 2008].

Liver fibrosis pathogenesis

Chronic liver disease (CLD) results in the development of chronic hepatic wound healing, which characterizes by persistent liver inflammation and accumulation of extracellular matrix proteins (ECM), collectively described as fibrosis [Bataller *et al*, 2005; Henderson *et al*., 2007]. Crucial players in the pathogenesis of liver fibrosis are hepatic stellate cells (HSCs) and macrophages [Friedman, 2008; Li *et al*., 2016]. HSCs, also termed Ito cells, are the pericytes of the liver, reside in the peri-sinusoidal space between endothelial cells and hepatocytes -space of Disse. In their inactive physiological status, their cytoplasm contains vitamin-A lipid droplets and expresses desmin and the neural marker glial fibrillary acidic protein (GFAP) [Friedman, 2008]. In injured liver, quiescent HSCs transdifferentiate into fibrogenic myofibroblasts-like cells maintaining their activated status in response to paracrine and autocrine stimulation. This process implies the loss of lipid droplets and GFAP, *de novo* expression of α-SMA, acquisition of contractility, proliferation, and migration. The fibrogenic role of active HSCs resides in their acquired ability to synthesize and secrete large amount of ECM proteins (mainly collagens and fibronectin) and pro-fibrotic factors which progressively accumulate in the injured tissue [Puche *et al*., 2013], exacerbating fibrosis. If it is true that typically these cells are cleared upon injury and inflammation subsidence, during CLD persistent inflammation perpetuates myofibroblast activation resulting in the progressive accumulation of ECM in the liver [Novo *et al*., 2015]. CLD is closely associated with the enrichment of liver macrophages [Zimmermann *et al*., 2010], both resident Kupffer cells and those derived from infiltrating monocytes (which are recruited from the bone marrow -BM- to engraft within the liver adiacent to ductular reactions -DRs-). In chronic or severe liver injury, submassive hepatocyte death and impaired proliferative capacity of hepatocytes occur, which induce the expansion of liver progenitor cells.

During the process of LPC-mediated regeneration, the hepatocytes give rise to duct-like progenitors that then differentiate back into mature functional hepatocytes. Macrophage or stellate cells in LPCs niche participate in directing the fate of LPCs. Moreover, they perform a diversity of functions during hepatic wound healing [Thomas *et al*., 2011], promoting inflammation and fibrosis by secreting a myriad of pro-inflammatory and pro-fibrotic factors (including TGFβ, PDGF, IL-1, IL-6, TNFα and TWEAK), in addition to promoting the recruitment of other immune cell populations and the clearance of cell debris by phagocytosis [Li *et al.*, 2016]. Unfortunately, all together these factors perpetuate inflammation, stimulate and maintain myofibroblast activation, and induce immune-mediated tissue injury [Gieling *et al*., 2009; Fielding *et al*., 2014; Yang *et al*., 2015; Tsutsui *et al*., 2015]. These activities perpetuate fibrosis which can eventually develop into cirrhosis. It is worth noting that macrophages are also associated with fibrosis amelioration through MMP-12- and MMP-13-mediated ECM degradation and through killing of HSCs by TRAIL. However the depletion of macrophages during the recovery phase causes the persistence of fibrosis through the promotion of HSCs survival and up-regulation of TIMP-1 [Duffield *et al*., 2005; Thomas *et al*., 2011; Sica *et al*., 2014; Seki *et al*., 2015]. Much of what we know about fibrosis pathology and potential treatments has been gathered from *in vivo* animal models of chronic tissue damage. Experimental models of hepatic fibrosis in rodents, dogs, and monkeys, whereby tissues were analyzed for collagen deposition have been fundamental for studying in particular the onset and pathogenesis of this disease (Table 1).

Models of liver fibrosis	Animal	Protocol/method	Onset of fibrosis
Toxic/xenobiotics			
Carbon tetrachloride (CCl_4)	Rats	s.c. or i.p. twice weekly, 0.2 ml/100 mg body weight of CCl_4 in oil (1:1 ratio)	>4–6 weeks
	Mice	i.p., every 5 days, 1 µl/g body weight of CCl_4 in oil (1:7 ratio)	4 weeks
Dimethylnitrosamine (DMN)	Rats	i.p., 10 mg/kg body weight, twice weekly	>4 weeks
	Mice	i.p., 10 mg/kg body weight, thrice weekly	>3 weeks
	Dogs	Orally twice weekly or intraportally once weekly	>3–6 weeks
Thioacetamide (TAA)	Rats	At 300 mg/l in drinking water	>2–3 months
	Mice	At 200 mg/l in drinking water	>3–4 months
		i.p., thrice weekly, 150–200 mg/kg body weight	>6 weeks
3,5-Diethoxy-carbonyl-1,4-dihydrocollidine (DDC)	Mice	Supplemented (0.1%) in solid diet	>4–8 weeks
Ethanol	Rats	Intragastric infusion of ethanol (25%–47% of calories) and high-fat diet	>3 months
	Mice	Liquid diet with 5% ethanol for 10 days, then 1 dose 5 g/kg body weight by gavage	Damage, no overt fibrosis
	Baboons	Liquid diet with ethanol (50% of calories), twice a day	>6 months
Nutritional			
Choline-deficient, ethionine-supplemented (CDE) diet	Mice	Choline-deficient diet supplemented with 0.15% ethionine in drinking water	>2 weeks
	Rats		>10 weeks
Methionine- and choline-deficient (MCD) diet	Mice	Methionine- and choline-deficient diet	8–10 weeks
	Rats		10 weeks
Methionine- and choline-deficient, ethionine-supplemented (MCDE) diet	Mice	Methionine- and choline-deficient diet supplemented with 0.15% ethionine in drinking water	1–3 weeks
Surgical			
Bile duct ligation	Mice	Common extrahepatic bile duct is ligated	3 weeks
	Rats		>4 weeks
	Dogs		>4 weeks
	Monkeys		>8 weeks
Genetic			
TGF-β1	Mice	Dox-repressible expression of TGF-β1 transgene, conditional to hepatocytes (*Cebpb-tTA*)	10 inductions
	Mice	LPS-inducible expression of fusion transgene CRP-TGF-β1, conditional to hepatocytes	Only mild fibrosis
Pdgfb	Mice	Expression of *Pdgfb* transgene, conditional to hepatocytes (albumin promoter)	>5 months postnatally
Mdr2 KO	Mice	KO of the phospholipid transporter *Mdr2*	>3 months postnatally
Nemo KO	Mice	KO of the NF-κB essential modulator (*Nemo*) conditional to liver parenchymal cells (*Alfp-Cre*)	>6–12 weeks postnatally
Tak1 KO	Mice	KO of TGF-β–activated kinase 1 (*Tak1*) conditional to liver parenchymal cells (*Alfp-Cre*)	>6–12 weeks postnatally
Bcl-xl KO	Mice	KO of the antiapoptotic *Bcl-xl* conditional to hepatocytes (albumin-*Cre*)	>5 months postnatally
Mdm2 KO	Mice	β-Naphthoflavone–inducible KO of *Mdm2* conditional to hepatocytes (*Ah-Cre*)	>3 months
Immunological			
2-OA-BSA/α-GC	Mice	Immunization with 2-octynoic acid and BSA, then exposure to α-galactosylceramide	>4–12 weeks

Table 1. Experimental animal models of liver fibrosis [in Cordero-Espinoza *et al*., 2018, *modified*]

As the injury becomes chronic, the hepatic parenchyma is overtaken by an acellular mesh of connective tissue, mostly collagen and elastin fibers, whose progressive cross-linking restrains access to degrading enzymes and makes scar resolution increasingly difficult [Ramachandran *et al*., 2012]. Unfortunately, in humans advanced liver fibrosis is much less reversible due to the decades, not weeks, of tissue damage and collagen cross-linking [Desmet *et al*., 2004]. Even after accounting for the variable of time, we cannot rule out species-specific differences in regeneration that may hinder our ability to treat patients. Thus, it may be time for the field to develop innovative human models of liver fibrosis.

Hepatic fibrotic extracellular matrix

Liver ECM proteins are mostly detected in the Glisson's capsule, portal tracks, central veins, and in the sub-endothelial space of Disse [Bedossa *et al*., 2003]. In chronically damaged livers, the vicious cycle of cell death, inflammation, and excessive ECM deposition overrides epithelial restoration.

Liver fibrosis is associated with major alterations in both the quantity and composition of extracellular matrix including collagens (I, III and IV), fibronectin, elastin, laminin and proteoglycans, among others. Also ECM-degrading enzymes known as matrix metalloproteinases (MMPs) have a key role in fibrosis dynamics. MMPs are calcium-dependent zinc-containing peptidases and are responsible for the degradation and turnover of most components in the ECM, including collagen [Duarte *et al*., 2015]. Moreover, MMPs are also involved in the regulation of immune responses. MMP activity can be regulated at multiple levels [Fanjul-Fernandez *et al*., 2010]. Additionally, cells can secrete tissue inhibitors of matrix metalloproteinases (TIMPs) that inhibit the activity of MMPs outside the cell. Different MMPs are inhibited by different TIMPs in a complex interaction network and therefore the specific balance of MMPs with their cognate TIMPs dictates the activity of the extracellular MMP pool. For example, TIMP-1 reacts with the zymogen form of MMP-9 [Vempati *et al*., 2007]. The pathological state of fibrosis is associated with an increased matrix stiffness due to the altered ECM composition, HSC-mediated remodelling, with stiffness dependent on both collagen amount and cross-linking [Wells, 2013]. This increased rigidity is detected by HSCs through cell surface receptors known as integrins [Desai *et al*., 2016]. The matrix remodelling proteins MMP-2 and 9 are two key MMPs secreted from HSCs that degrade collagen [Bonnans *et al*., 2014], and a sensitivity of MMP and TIMP secretion by HSCs to external rigidity underlies an important feedback loop regulating the composition of the ECM in fibrosis. In particular, MMP9, which breaks down collagen, is reported to exert an anti-fibrotic effect in murine models of chronic liver injury [Duarte *et al*., 2015]. An overview of the state of hepatic parenchyma under chronic injury is reported in Figure 2.

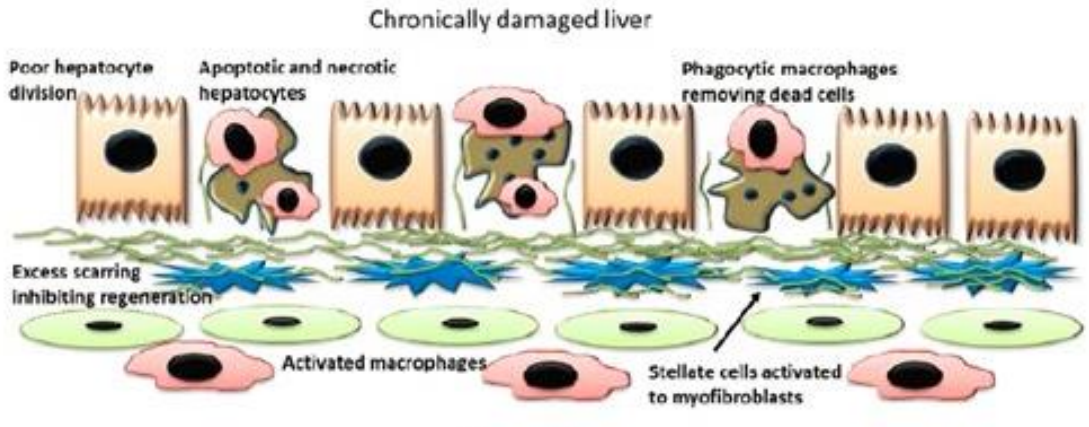

Figure 2. Representation of an abnormal chronically damaged liver. Hepatocytes are senescent and unable to divide efficiently, the stellate cells are in their active form and excessive scar tissue inhibits regeneration. Excessive cellular debris inhibits efficient liver regeneration [in Forbes *et al*., 2019, *modified*].

Liver Regeneration

In an elegant study by Li and colleagues published in 2010, the *Phoenix rising pathway* is proposed to sustain the intriguing point of view that dying cells (cells in apoptosis, more precisely) in the wounded tissues send signals through caspases to stimulate the proliferation of stem or progenitor cells to start the process of tissue regeneration and wound healing [Li *et al*., 2010] (Figure 3).

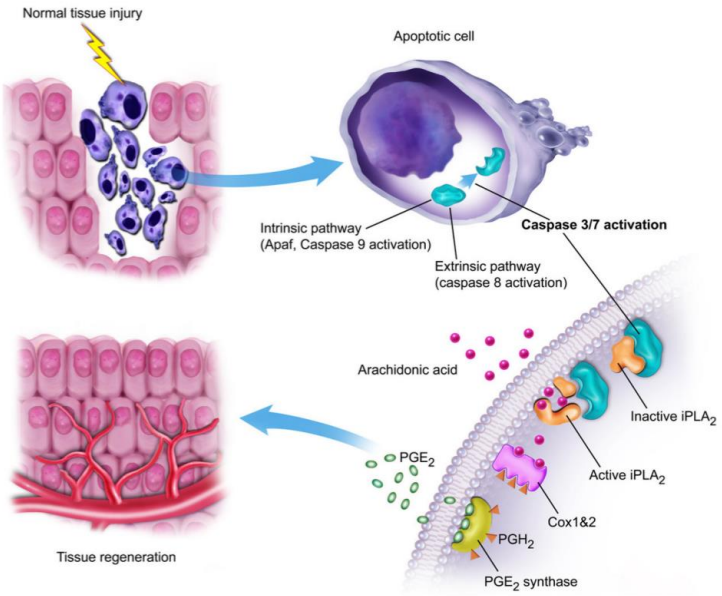

Figure 3. The Phoenix rising pathway [in Li F. *et al*., 2010]

Mammalian organs have a limited regeneration potential, with the exception of the liver. Following injury, the liver is able to mount a dynamic multicellular response wherein stromal cells activated in situ or are recruited from the bloodstream, the ECM is remodeled, and epithelial cells expand to replenish their lost numbers. With a chronic damage this response becomes persistent instead of transient, overturning the system into an abnormal steady state known as fibrosis, in which ECM accumulates excessively and tissue function degenerates. [Cordero-Espinoza *et al*., 2018]. The most effective therapy for treating liver fibrosis to date is still to remove the damaging agent. Liver contains built-in mechanisms for scar resolution which inactivated in the face of unceasing damage. The removal of pro-fibrotic inputs or the strengthening of anti-fibrotic ones, should then stimulate scar resolution to some extent. At the ground level, the battle is enzymatic. In fact, as the injury becomes chronic, the once-functional hepatic parenchyma is overtaken by an acellular mesh of connective tissue whose progressive cross-linking restrains access to degrading enzymes and makes scar resolution increasingly difficult [Ramachandran *et al*., 2012, a]. Matrix-degrading enzymes must overcome the inhibitory action of TIMPs for a scar to be broken down. Overexpression of enzymes like MMP1 and MMP8 through adenoviral delivery has proven to ameliorate established fibrosis in rat livers [Iimuro *et al*., 2003]. Compounding the problem is the chronic persistence of

myofibroblasts, which continuously pump TIMPs into the microenvironment, owing to pro-survival signaling via TGF-β and the TNF-α/NF-κB axis [Saile *et al*., 1999]. The cessation of healing is albeit a process that is poorly understood. In fibrosis resolution, then, increased activity of MMPs leads to collagen degradation and ECM softening, with consequent reversion of activated HSCs to their quiescent phenotype [Lachowski *et al*., 2019]. In this scenario a pivotal role is also played by the infiltrating immune component. Increased numbers of dendritic cells (DCs) [Jiao *et al*., 2012], NK cells [Krämer *et al*., 2012] and macrophages [Ramachandran *et al*., 2012, b] arrive in the tissue parenchyma. While DCs directly target ECM degradation through MMP9 secretion [Jiao *et al*., 2012], NK cells target activated and senescent myofibroblasts for apoptosis through IFN-γ–induced NKG2-D type II integral membrane protein (NKG2D), TRAIL, and FasL [Radaeva *et al*., 2006]. T cells expressing the γδ T cell receptor can also induce myofibroblast apoptosis via the Fas/FasL axis and thereby limit hepatic fibrosis [Hammerich *et al*., 2014]. In Figure 4 landscapes characterizing fibrosis and resolution in the liver are depicted.

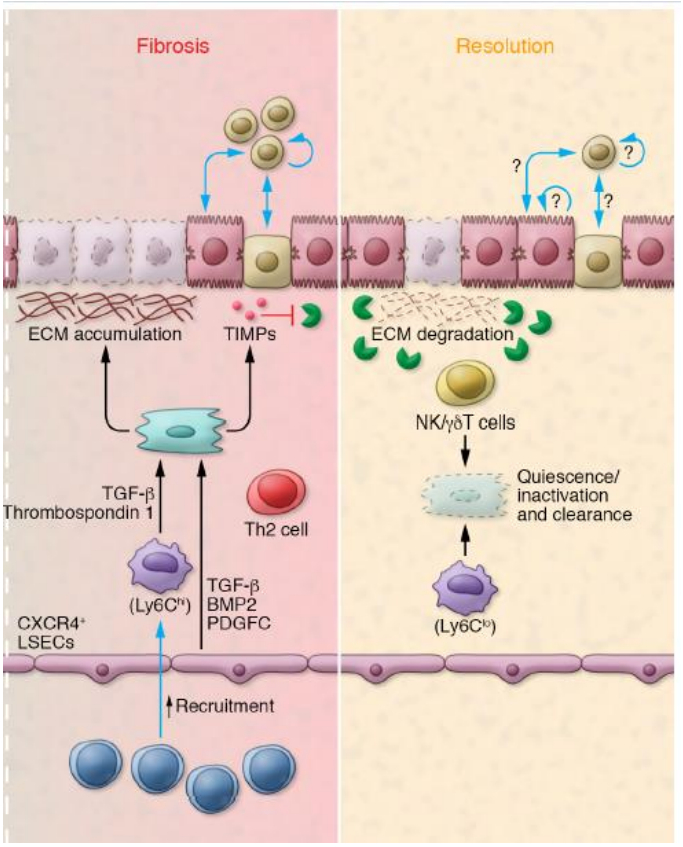

Figure 4. Landscapes characterizing fibrosis and resolution in the liver. In fibrosis, the hepatocyte compartment is highly senescent and ductal progenitor expansion becomes predominant. Monocyte-derived Ly6Chi macrophages (secreting TGF-β) and CXCR4^{+} LSECs (secreting TGF-β, BMP2, and PDGFC) enhance myofibroblast proliferation and survival. Myofibroblasts, in turn, secrete high levels of TIMPs, which inhibit MMPs and cause excessive matrix accumulation. A Th1- versus Th2-skewed immune system favors regeneration versus fibrosis, respectively. The resolution of fibrosis

entails the return to quiescence/inactivation of myofibroblasts as well as their clearance by NK cells, γδ T cells, and Ly6C^{lo} macrophages. High levels of MMPs contribute to matrix degradation. The mechanisms of epithelial replacement at this stage have not been fully elucidated [in Cordero-Espinoza *et al*., 2018, *modified*].

How to study hepatic regeneration and repair: animal models

In the biological field, the liver is the only visceral organ able the ability to regenerate after partial resection or chemical injury. This feature is defined compensatory hypertrophy (cell size increase) followed by hyperplasia (cell number increase) of remaining hepatocytes to compensate for the lost tissue, restore the full liver size, and meet the metabolic needs of the organism without regaining its original anatomical gross shape. This process is neither a new creation of the missed tissue nor a true anatomical regeneration because it does not follow the steps of the true regenerative process particularly the blastema formation. Therefore, this phenomenon should be properly termed as compensatory liver hyperplasia rather than liver regeneration. However, we use the term "liver regeneration" is significantly mentioned in the scholarly literature [Fausto *et al*., 2006; Mao *et al*., 2014; Rmilah *et al*., 2019]. An important clinical scenario where an improved understanding of regeneration of the compromised liver is mandatory includes liver transplantation, where is increasingly common the use of split livers and living donor transplants rely upon regeneration of the donor graft to reach the correct liver mass. Failure of regeneration in these settings results in poor or delayed graft function, prolonged intensive care stays, occasionally a requirement for re-transplantation or ultimately even death of the recipient [Forbes *et al*., 2019].

Multiple animal models have been studied to describe and investigate the liver regeneration process. Basically all the published models fall within the following macro-groups:

1. Rodent surgical partial hepatectomy (PH) model. This model, well described in a landmark paper in 1931 by Higgins and Anderson [Higgins *et al*., 1931] has been deeply exploited in rodent representing the best choice for many researchers. As reported in Figure 5, it contemplates a surgical removal of the left lateral, left medial and right medial lobes leaving the right lateral and caudate lobes, with a more than 50% decrease in the liver size. Whilst the normal adult liver is mitotically quiescent with only minor hepatocyte proliferation detectable, following resection, the remaining hepatic tissue proliferates and expands in size to retain the original mass of five lobes within 5–7 days, undergoing a series of rapid vascular endothelial, inflammatory and epithelial changes. The peak of proliferation is after 24 h in rat whereas, in mice, it is between 36 h and 48 h [Mao *et al*., 2014; Michalopoulos, 2007]. The high success of this model relies on the ability of the surgical operator to resect with high accuracy due to the uniformity of the rodent's liver anatomy and on the fact that the procedure is a simple operation that does not require an advanced

surgical technique. Moreover the procedure is well tolerated in rodents without any significant perioperative mortality and it is not associated with any histological damage or injury to the residual liver tissue. The accuracy of timing of the sequence of subsequent events that can be observed from the first 5 min to 5–7 days [Mao *et al*., 2014; Michalopoulos, 2007; Pritchard *et al.*, 2015].

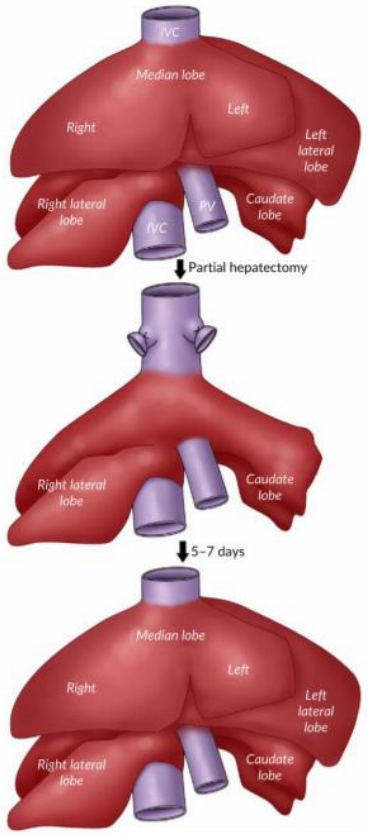

Figure 5. Partial hepatectomy [in Rmilah *et al*., 2019]

2. Rodent and mice chemical-induced hepatotoxic injury or pharmacological models (carbon tetrachloride, D-galactosamine, acetaminophen or paracetamol). The liver has the capability to regenerate after a chemical-induced injury. Differently from PH model, the pharmacological model is easier to be executed as it induces a necrotic injury that simulates certain liver diseases. These properties made the model an acceptable option to study liver regeneration. The main drawback of this model is the poor liver reproducibility and standardizability, if the operator has not a high expertise with this issue. In particular, the difficulty to expect the degree of liver injury and regeneration and avoid substantial differences between experiments; namely, raising the toxin concentration can induce acute liver injury while repeated administration of the toxin can lead to liver cirrhosis. Moreover, the systemic and local effects of the toxin depend on route and dose of administration, animal species including their age and nutritional status [Mao *et al*., 2014;

Michalopoulos, 2007; Palmes *et al*., 2004; Pritchard *et al.*, 2015]. The most employed and published hepatotoxins in liver regeneration models are the following. *Carbon tetrachloride* (CCl_4), a volatile organic and hepatotoxic compound which induces an acute liver injury after its breakdown by cytochrome P450 2E1 (CYP2E1) leading to the formation of highly reactive and toxic radicals: trichloromethyl (CCl3*) and trichloromethylperoxy (CCl3OO*) radicals. These metabolites trigger an oxidative damage to DNA, proteins, lipids, and carbohydrates in hepatocytes causing their necrosis. It is also accompanied by stimulation of KCs that produce more oxygen free radicals and cytokines, thus contributing more to the cell damage. These events induce an acute inflammatory response represented by polymorphonuclear leukocytes and macrophages to remove necrotic debris of hepatocytes. This type of injury is a reversible acute hepatic injury, followed by liver regeneration because it was observed that an extreme elevation in plasma ALT activity in mice takes place within 36 h, and then it reduces to more than 90% of 36 h level by 72 h after CCl_4 exposure. It is associated with centrilobular necrosis in the pericentral area -zone 3- where the CYP2E1 is highly concentrated [Mao *et al*., 2014; Michalopoulos, 2007; Pritchard *et al*., 2015]. *D-galactosamine*, considered as a strong hepatotoxic compound, it causes an acute liver failure altering the metabolic system in the liver leading to depletion of uridine triphosphate and thus inhibition of RNA and protein synthesis. Moreover, D-galactosamine contributes to the inflammation and necrosis of liver cells promoting the intestinal mast cell degranulation that represses the intestinal protection barrier, hence allowing more endotoxins to reach the portal circulation to the liver. The sequence of regenerative events occurs at the same time as that for CCl_4, however, the liver regenerative capacity of this model is weaker than that of CCl_4 model [Mao *et al*., 2014; Palmes *et al*., 2004; Pritchard *et al*., 2015]. *Acetaminophen or* paracetamol, a well-known antipyretic medication, has a toxic effect following overdose, clinically manifested as fulminant acute hepatic failure. This model is deeply exploited in mice to study the mechanisms of acute liver injury. Administration of supra pharmacological toxic dose of acetaminophen overwhelms the physiological metabolizing reactions in the liver leading to the accumulation of toxic metabolite called N-acetyl-benzoquinone imine. Subsequently, the formation of radicals and cytokines along with KC activation are the main pathological issues that ensue an acute inflammatory reaction and cell necrosis. The processes underlying the liver regeneration of this toxic model are relatively less comprehended than other models. Therefore, additional experiments should be performed to study the liver regeneration in the context of acetaminophen overdose [Mao *et al*., 2014; Palmes *et al*., 2004; Pritchard *et al*., 2015].

3. Zebrafish. This animal model is relatively recent and it has been developed to model many diseases and understand pathophysiological processes [Cox *et al*., 2015]. The small size and optical translucency brings the advantages of low cost and rapid analysis. To date, literature demonstrates that many of the biological processes and signalling pathways seen in mouse and rat are recapitulated in zebrafish. There are a number of ways of provoking liver regeneration in the zebrafish including surgical partial hepatectomy and drug induced liver injury. The zebrafish has a trilobar structure and the one-third partial hepatectomy model has been established in the zebrafish by removal of one lobe [Sadler *et al*., 2007]. Clearly this is currently a more limited resection than performed in rodents. These studies have established signals such as Wnt, BMP and FGF as important for liver regeneration in zebrafish [Goessling *et al*., 2008; Vliegenthart *et al*., 2014]. Interestingly zebrafish exhibit cellular plasticity in that bile ducts can convert to hepatocytes following large-scale hepatocyte loss. Two independent reports found, using hepatocyte ablation and lineage tracing, that following extensive hepatocyte loss the biliary cells are able to regenerate the hepatocytes [He *et al*., 2014; Verfaillie, 2014]. Interestingly, in an ethanol induced model of liver fibrosis Huang and coworkers found that Wnt and Notch have opposing roles in directing HPCs in their regeneration of hepatocytes. Low levels of Notch stimulation stimulated HPC proliferation and hepatocyte differentiation, high levels of Notch suppressed this pathway. Wnt ligands were found to suppress Notch signalling via Numb, a protein inhibitor of Notch [Huang *et al*., 2014]. Importantly this helps to validate the zebrafish model in the liver regeneration setting, as the same opposing signals Wnt and Notch acting via the node Numb signals have previously been shown to control the behaviour of HPCs in mouse and are differentially expressed in hepatocellular versus biliary injury in human liver [Boulter *et al.*, 2012]. Zebrafish are an ideal model for "forward genetic" due to their small size and ability to screen large numbers of organisms following exposure to a chemical mutagen. Phenotypes can be screened and the actual gene/s responsible then mapped, an approach that has already yielded results in the setting of liver development [Jiang *et al*., 2015]. This exciting new model system looks set to make important inroads especially into the area of screening compounds for their effects upon liver regeneration. However some caution needs to be expressed, and it is important to translate identified signals and targets into mammalian systems -including human- for liver regeneration [Forbes *et al*., 2019].

4. Recently, genetically modified animal models have been extensively employed in the research field of liver regeneration. Several models have been established such as a mouse model developed by Grompe and collaborators in 2007 [Azuma *et al*., 2007]. This model is a triple-knockout model immunodeficient due to the silencing of Rag2 and II2rg genes, with hereditary tyrosinemia because

of fumarylacetoacetate hydrolase (FAH) deficiency. Silencing of FAH gene prevents the production of FAH protein which plays an essential part in the tyrosine metabolism by catalyzing the conversion of fumarylacetoacetate into fumarate and acetoacetate, the last step of tyrosine metabolism. As a result the tyrosine accumulates in the liver of mouse causing acute liver failure. Another interesting transgenic mouse model is the one known as CD11b-DTR transgenic mouse, in which the selective depletion of macrophages is possible [Duffield *et al*., 2005], to study *in vivo* macrophage function in relation to fibrosis dynamics and liver regeneration. Here a conditional ablation system mediated by diphtheria toxin (DT) receptor is exploited [Saito *et al.*, 2001]. This system relies on the fact that the mouse DT receptor (heparin-binding EGF; hbEGF) binds DT poorly compared with the human molecule (27). Thus, transgenic expression of the human DT receptor (DTR) confers sensitivity to DT and permits macrophages ablation *in vivo* when DT is injected. By means of this transgenic mouse model it was demonstrated the critical and somehow opposite function of macrophages accordingly to the precise moment in which they act. Macrophage depletion when liver fibrosis was advanced resulted in reduced scarring and fewer myofibroblasts. Macrophage depletion during recovery, by contrast, led to a failure of matrix degradation. With their work, Duffield and collaborators demonstrated for the first time that functionally distinct subpopulations of macrophages exist in the same tissue and that these macrophages play critical roles in both the injury and recovery phases of inflammatory scarring.

Aims

We recently demonstrated in mice that after an acute liver damage induced by a single injection of the toxin CCl_4, a dimorphic recruitment of infiltrating monocyte subset $CD11b^{high}Gr\text{-}1^{high}$ macrophages represented a key factor affecting liver architecture restoration in a different manner between males and females [Bizzaro *et al*., 2018].

Considering this aspect and since the mechanisms regulating fibrogenesis and regeneration are under lively investigation, with this PhD thesis the attention was moved on a chronic setting of hepatic injury, where a relentless damage CCl_4-mediated was established in Balb/cJ mice, either males or females.

Our interest was to investigate if also in a chronic model of liver injury the processes of fibrogenesis and fibrinolysis were differently regulated in males and females mice. The ultimate goal is to clarify the implications of gender differences in promoting the fibrogenic and regenerative response to chronic liver damage.

Through an exploration both in males and females mice of the cellular and molecular events which switch that balance between hepatic fibrosis and restoration, we focus in particular on uncovering avenues characterizing differently the microenvironment, both hepatic and circulating, according to gender.

Methods

Ethics Statement

The procedures involving animal care followed institutional guidelines that comply with national and international laws and policies (European Economic Community Council Directive 86/609, OJL 358, 1 Dec. 2012, 1987; NIH Guide for the Care and Use of Laboratory Animals, NIH Publication no. 85-23, 1985). The study design was approved by the Ethics Committee of the University of Padova for the care and use of laboratory animals (CEASA protocol number 108288/2013, approved by the Ethics Committee of the University of Padova, Italy)

Animals

Female and male Balb/cJ mice 6 week-old were purchased from Charles River (Charles River Laboratories International Inc., Wilmington, Massachusetts, USA). Animals were maintained in a pathogen-free and temperature-controlled environment at 12h light/dark cycle and were fed with a standard rodent diet and water a*d libitum*. Special attention to enrichments was paid for animals welfare.

Experimental design of the injury model

The model of chronic hepatic injury was established by intra-peritoneal injection of a 1:7 mixture of CCl_4 (Sigma-Aldrich, Milan, Italy) in olive oil, at a dose of 1.2 μL/g body weight, twice a week, for 12 weeks. Mice were randomly divided into carbon tetrachloride (CCl_4)-treated (n=5/each time point/gender) and olive-oil treated (controls mice; n=5/ each time point/gender) groups. A group of not-treated animals was included in the study for kinetics of growth evaluation throughout the experiments. The treatment was well tolerated by animals, as confirmed by absence of death during the treatment and also by growth curves (Figure 6).

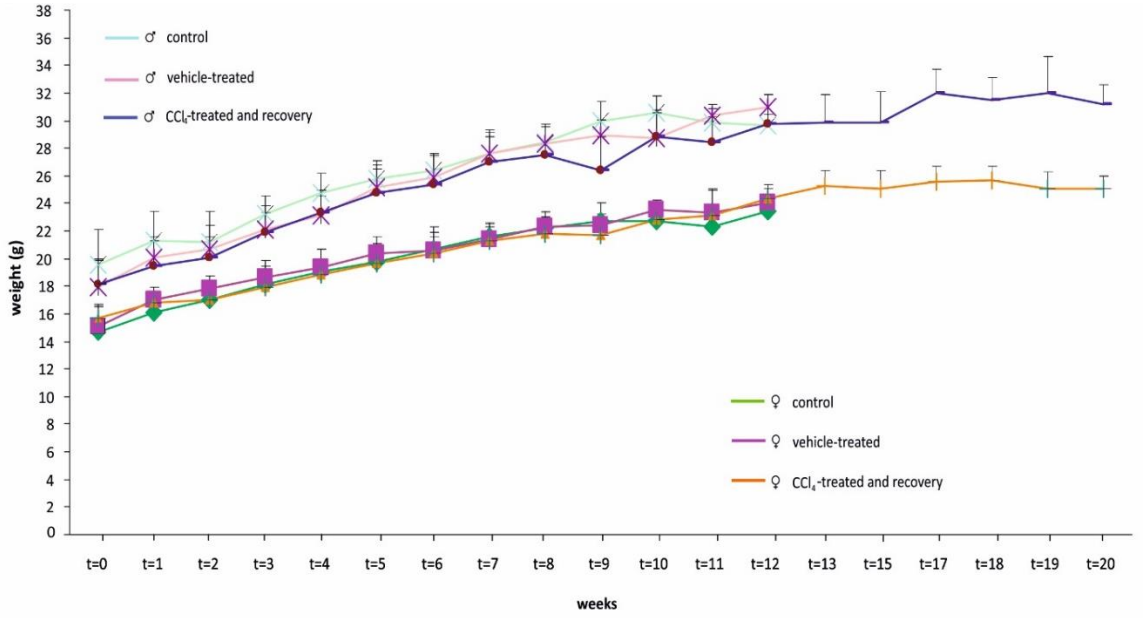

Figure 6. The kinetic of growth of animals included in the study evaluated for the entire period of repeated CCl_4 administration and after the self-healing. Weights of animals were expressed in grams (g) as mean±sd.

Animals were euthanized at week 2, 6, 12 from the beginning of the treatment and after 8 weeks from the end of the intoxication (this group is defined recovery from here forward), during which animals were left to self-heal the liver (Figure 7). All biological materials were properly harvested from animals painless sacrificed 72 hours after the last injection of CCl_4.

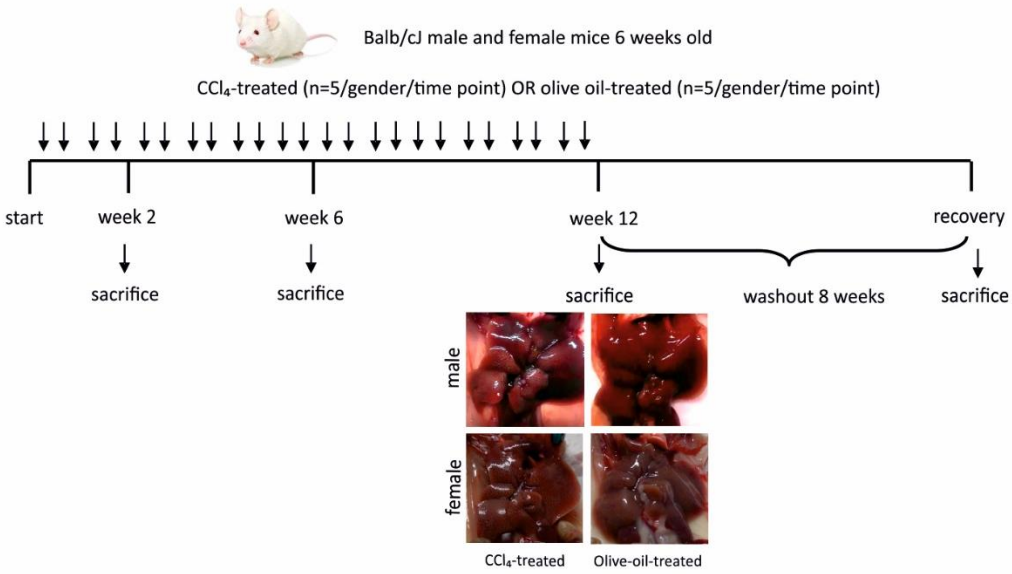

Figure 7. Experimental Design of the model of injury developed in this study. Balb/cJ mice, either male or females, 6 weeks-old, were randomly divided in two groups: one receiving 1 µL/g of a mixture 1:7 of CCl_4 in olive oil, the other 1 µL/g of olive oil, twice a week for 12 weeks. A group of animals was observed also for 8 weeks after the last CCl_4 injection. Animals were euthanized at week 2, 6, 12 after the beginning of the protocol and after the 8-weeks period of self-healing. Representative macroscopic images of the liver at the end of the protocol are reported.

Histological analysis, Immunohistochemistry and signal quantification

As soon as animals were euthanized, livers were perfused with PBS. Mouse liver tissues dedicated to histology were then immediately fixed in 10% buffered formalin and processed for paraffin embedding. Five-µm thick sections were then stained with Haematoxylin-Eosin (H-E, Diapath Spa, Martinengo, BG, Italy), Sirius Red staining (Bio-Optica spa, Milan, MI, Italy) or by immunohistochemistry –IHC- for the following epitopes: alpha-SMA, F4/80, Asp-175, CK-7. The IHC set-up conditions are summarized in Table 2.

Epitope	**Function**	**Company**	**Clone**	**Code**	**Conditions**
alpha-SMA	HSCs activation	Sigma	1A-4	A5228	1:2000 overnight at 4°C
F4/80	Activated macrophages	Abcam	SP115	#ab111101	1:100 overnight at 4°C
Asp-175	Caspase 3 clivation for apoptosis evaluation	Cell Signaling Technology	Not applicable	#9661	1:300 overnight at 4°C
CK-7	Progenitor cell/biliary cell phenotype	Abcam	RCK105-	#ab9021	1:1000 overnight at 4°C

Table 2. Specifications for antibodies used and set-up conditions in immunohistochemistry experiments

The quantification of signals was performed as follows:

1. Fibrotic areas (Sirius Red staining) for each group were quantified as a mean±SE of a ratio between the sum of all Sirius Red$^+$ areas per slide [µm^2] and total area of the liver section in the slide [µm^2] (at 100x magnification).

2. For HSCs activation, the amount of alpha-SMA$^+$ areas was calculated as mean±SE of a ratio between the sum of all alpha-SMA$^+$ areas per slide [µm^2] and total area of the liver section in the slide [µm^2] (at 100x magnification).

3. The evaluation of apoptotic cells was performed by counting 6 fields/slide at 400x HPF. For each field both the number of Asp-175$^-$ cells (haematoxylin$^+$ nuclei) and Asp-175$^+$ cells were counted. A ratio between Asp-175$^+$ cells and total counted cells was calculated. Then the final value of Asp-175$^+$ cells was a mean±SE of the values calculated for each slide per each experimental group.

4. The evaluation of CK7$^+$ was performed by counting 6 fields/slide at 400x HPF. For each field both the number of CK7$^-$ cells (haematoxylin$^+$ nuclei) and CK7$^+$ cells were counted. A ratio between CK7$^+$ cells and total counted cells was calculated. Then the final value of CK7$^+$ cells was a mean±SE of the values calculated for each slide per each experimental group.

5. The evaluation of F4/80^{+} was performed by counting 6 fields/slide at 400x HPF. For each field both the number of F4/80^{-} cells (haematoxylin^{+} nuclei) and F4/80^{+} cells were counted. A ratio between F4/80^{+} cells and total counted cells was calculated. Then the final value of F4/80^{+} cells was a mean±SE of the values calculated for each slide per each experimental group.

RNA isolation

Mouse liver specimens were cut into small pieces, immediately snap frozen in liquid nitrogen, then stored at −80°C. Liver specimens (5-10 mg) were homogenized by means of Polytron (KINEMATICA AG, Luzern, Switzerland) in 1 mL of TRIzol (Life Technologies Corporation, Carlsbad, USA) and total RNA was subsequently extracted according to the manufacturer's instructions. RNA concentrations were quantified spectrophotometrically by means of Nanodrop 2000 (Thermo Scientific, Wilmington, Delaware USA). The quality of the RNA isolated was assessed using the RNA 6000 Nano Assay and the Agilent 2100 bioanalyzer (Agilent Technologies, Palo Alto, CA, USA).

Real-Time PCR

Five hundred ng of RNA were reverse transcribed in a final volume of 20 μL in the presence of SuperScript™ IV VILO™ Master Mix (Thermo Scientific) or SuperScript™ IV VILO™ Master Mix "No RT" control which was used as blank. The annealing of primers was performed at 25°C for 10 min; the reverse transcription of RNA was performed at 50°C 10 min with a final step of enzyme inactivation at 85°C for 5 min. The instrument used was a Perkin Elmer GeneAmp PCR System 2400. The cDNA was stored at −20°C. Real-time polymerase chain reaction for the study of gene expression modulation of MMP9 and MMP13, CXCL9, VEGFA, IL-6 and IL-12β, was conducted in an ABI 7900 HT Sequence Detection System (Applied Biosystems, Foster City, CA, USA) using a Taqman Fast Advanced Master Mix (Thermo Scientific). The reaction was performed in 96-well plates, in a 20μL final volume containing 1 μL of Taqman gene expression assay, 10 μL of Taqman Fast Advanced Master Mix, 5 μL of RNase free water and 4 μL of 2.5 ng/μL cDNA template. Samples in which the cDNA was omitted were used as negative controls. After one 2 min step at 50°C and a second step at 95°C for 2 min, samples underwent 40 cycles of 1 s at 95°C and then 20 sec at 60°C. For the determination of the relative concentration, gene expression was normalized to GAPDH calculated by the change-in-cycling-threshold method as $2^{-\Delta\Delta C(t)}$. All tests were performed in duplicate for each sample. Results are presented relative to those of mRNA of control oil-treated male mice, set as 1. FAM-MGB Taqman gene expression assays (Thermo Scientific) for mouse MMP9 (assay ID: Mm00442991_m1, amplicon length 76 bp), MMP13 (assay ID: Mm00439491_m1,

amplicon length 65 bp), CXCL9 (assay ID: Mm00434946_m1; amplicon length 64 bp) VEGFA (assay ID: Mm00437306_m1; amplicon length 61 bp), IL-6 (assay ID: Mm00446190_m1, amplicon length 78 bp), IL-12β (assay ID: Mm01288989_m1, amplicon length 63 bp), and GAPDH (assay ID: Mm99999915_g1, amplicon length 109 bp) were chosen.

Western Blot

For the analysis of IL-6, VEGFA, Collagen I-III-IV, TIMP-1 and CYP2E1 by Western Blot, mouse liver specimens (5 mg) were homogenized by means of Polytron (KINEMATICA AG) in 700 µL of RIPA Lysis Buffer ice cold (Sigma Aldrich, St Louise, Missouri, USA) with 1x Halt phosphatase and protease inhibitor cocktail (Thermo Scientific). Proteins were quantified by means of BCA method (Thermo Scientific), aliquoted and stored at -80°C. Twenty µg of proteic lysates were prepared for gel electrophoresis and protein transfer following manufacture instructions (Biorad, Hercules, CA, USA). The antibodies used for blotting are listened in Table 3.

Epitope	Company	Code	Clone	Conditions
IL-6 24 kDa	Abcam	ab191194	MP5-20F	1:400 overnight 4°C
VEGFA 45 kDa	Abcam	ab1316	VG-1	1:200 overnight 4°C
TIMP-1 23 kDa	Abcam	ab86482	RM0136-6A34	1:1000 overnight 4°C
Collagen I 139 kDa	Abcam	ab88147	3G3	1:1000 overnight 4°C
Collagen III 138 kDa	Abcam	ab7778		1:5000 overnight 4°C
Collagen IV 160 kDa	Abcam	ab52235		1:1000 overnight 4°C
GAPDH 38 kDa	Millipore	MAB374		1:1000 overnight 4°C
CYP2E1 57 kDa	Abcam	ab151544	EPR10078(B)]	1:1000 overnight 4°C
Calnexin 67 kDa	Santa Cruz	sc-11397	H-70	1:700 overnight 4°C

Table 3. Specifications for antibodies used and set-up conditions in western blot experiments

GAPDH was used as housekeeping protein, with the exception of CYP2E1, for which the housekeeping chosen was calnexin [Gabbia *et al*., 2017]. Signals were detected by means of Uvitec technology (Uvitec, Cambridge, United Kingdom) and results were expressed as a ratio of densitometric amount of protein of interest/protein housekeeping.

Gelatin Zymography for MMP9

To evaluate the gelatinolytic activity of MMP9 (active form: 82 kDa) present in the liver, 2 µg of proteic lysate samples were separated by electrophoresis in non-reducing conditions in 10% SDS-PAGE gel co-polymerized with gelatin 0.1%. After two washings with Triton X-100 (renaturing

phase), 30 min each, gel was incubated for 16 h at 37°C with collagenase buffer (Tris-HCl, 50 mM; NaCl, 200 mM; $CaCl_2$, 10 mM a pH 7.4). Then it was coloured with a solution of 30% methanol/10% acetic acid with 0.5% Coomassie Brilliant Blue R-250 (Amersham-Pharmacia, Milan, Italy) 1 h at room temperature and then de-coloured with a solution of 30% methanol/10% acetic acid. Positive controls were represented by serum-free conditioned media of HK2 cells which secrete the collagenase. Clear bands on blue background represent areas in which gelatin has been digested by MMPs present in the sample itself. Quantification was performed by densitometric analysis of the image (ImageJ software, http://rsb.info.nih.gov/ij/). Results were normalized relative to those of control oil-treated male mice, set as 1.

Flow Cytometry (FCM) analysis

As soon as animals were euthanized, livers were perfused with PBS, removed and properly processed for obtaining single-cell suspensions. In particular a solution of 0.05% w/V of collagenase IV and 0,005 µg/mL of DNAse (Sigma-Aldrich) in PBS (Sigma-Aldrich) was used to digest the minced liver for 15 min at 37°C. The suspension was then filtered by means of 40 µm-diameter Falcon® cell strainers (Corning, New York, USA), washed in PBS-10% FBS and centrifuged twice at 1200 rpm for 5 min. Five $x10^5$ cells/mL were incubated, according to manufacturer instructions, with anti-mouse F4/80 Antigen PE-Cyanine7 (eBioscience Inc., San Diego, CA, USA), FITC rat anti-mouse Ly6G (Gr-1) (eBioscience), PE rat anti-mouse GATA6 (Cell Signaling Technology, Leiden, The Netherlands), PeCy5.5 rat anti-mouse CD11c (eBioscience), Alexa Fluor 700 rat anti-mouse CD45 (eBioscience) and APC-eFluor 780 rat anti-mouse CD11b (eBioscience) and after 30 min incubation at RT in the dark, analysed on a Navios Flow Cytometer (Beckman Coulter, Milano, Italy). Relative percentages of different populations were calculated based on live $CD45^+$ gated cells (as measured by the physical parameters of side scatter and forward scatter). Preliminary analysis of unlabelled cells was used to verify antibody labelling specificity and the gating between positively and negatively stained cell populations. For $GATA6^+$ populations, a step of permeabilization, following manufacturer instructions, was included and the amount of cells was evaluated on both $CD45^+$ and $CD45^-$ gates. Data were expressed as absolute number of population of cells of interest and the expression level in control mice was used as the reference value.

Serum evaluation of estradiol and testosterone

Hormone assay. In collaboration with Dr. Annalisa Stefani (Istituto Zooprofilattico Sperimentale delle Venezie -IZSVe, Legnaro (Padova), Italy) the following analytes were measured. Serum levels of 17β-estradiol [pg/mL] (estradiol from here forward) and testosterone [ng/dL] were measured by

electro chemiluminescent immunoassay (ECLIA) methods on a Cobas e601 system (Estradiol III and Testosterone II, Roche Diagnostics GmbH, Mannheim, Germany) following manufacturer instructions. Performance data for each test are reported: for estradiol, analytical sensitivity of 5 pg/mL, intra-assay and inter-assay CV of 6.7% and 10.6 % respectively; for testosterone, analytical sensitivity of 2.5 ng/dL, intra-assay and inter-assay CV of 2.8% and 3.2 % respectively.

Multiplexed assaying of serum cytokines and chemokines

Two-fold diluted sera were evaluated for a multi-cytokines panel (GM-CSF, IFN-gamma, IL-1 alpha, IL-1 beta, IL-12 p70, IL-17A, IL-2, IL-4, IL-5, IL-6, IL-9, MCP-1/CCL2, M-CSF, RANTES/CCL5, TNF alpha, VEGFA) was performed by means of Mouse Cytokine Array Q1 Quantibody® array, a multiplexed sandwich ELISA-based quantitative array platform followed by the fluorescence detection with a dedicated laser scanner (QAM-CYT-1; RayBiotech, Norcross, GA), following manufacturer' instruction. The analysis of data was performed by Q-Analyzer, which is an array specific, Excel-based program. The Q-Analyzer Tool specific for this array is QAM-CYT-1-SW. Data are presented as mean±SE.

Statistics

The statistical difference among experimental groups was calculated using Mann-Whitney Rank Sum test or Student's t-test (after verifying normality of the distribution and the equality of variances). Differences were considered statistically significant for $p<0.05$. Data are expressed as mean±sd or mean±SE (where properly indicated).

Results

Fibrosis evaluation

Hepatic parenchyma was evaluated by H&E to confirm the establishment of the damage and to verify the presence of inflammatory infiltrate (Figure 8).

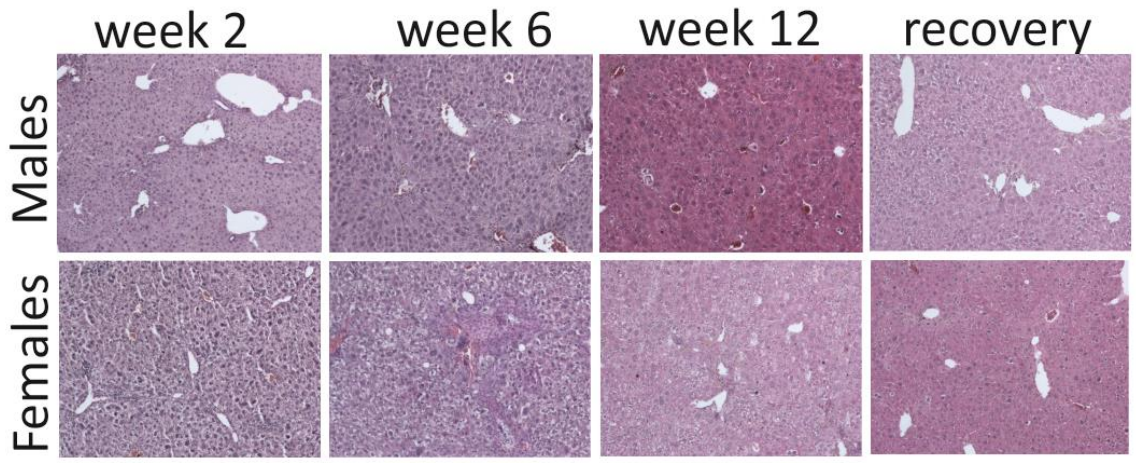

Figure 8. H&E representative images of males and females hepatic parenchyma at 2, 6, 12 weeks of CCl_4 treatment and after a self-healing of 8 weeks (recovery group). Magnification: x100.

To evaluate the extension of fibrotic parenchyma, livers of both males and females were Sirius Red stained. As evidenced in Figure 9, the amount of fibrosis at week 2 was significantly lower in female in respect to male mice (males *vs* females: 8.4±2.02 *vs* 5.52±1.01 p=0.021). At week 6 the fibrotic septa increased in both (males *vs* females: 9.26±4.07 *vs* 8.68±1.96 p=0.781). A statistical significant reduction in fibrotic area was observed at week 12 in female in respect to male animals (males *vs* females: 5.15±1.1 *vs* 2.63±0.95 p=0.005). Recovery group showed an almost regenerated architecture, even though porto-portal and porto-central fibrosis were present (Figure 9). However, even though animals were allowed to self-heal in the same conditions, the amount of fibrosis in the recovery group significantly differed between female and male mice. In particular, fibrosis in females was significantly higher compared to males (males *vs* females: 2.46±0.53 *vs* 4.48±1.39 p=0.032) (Figure 9).

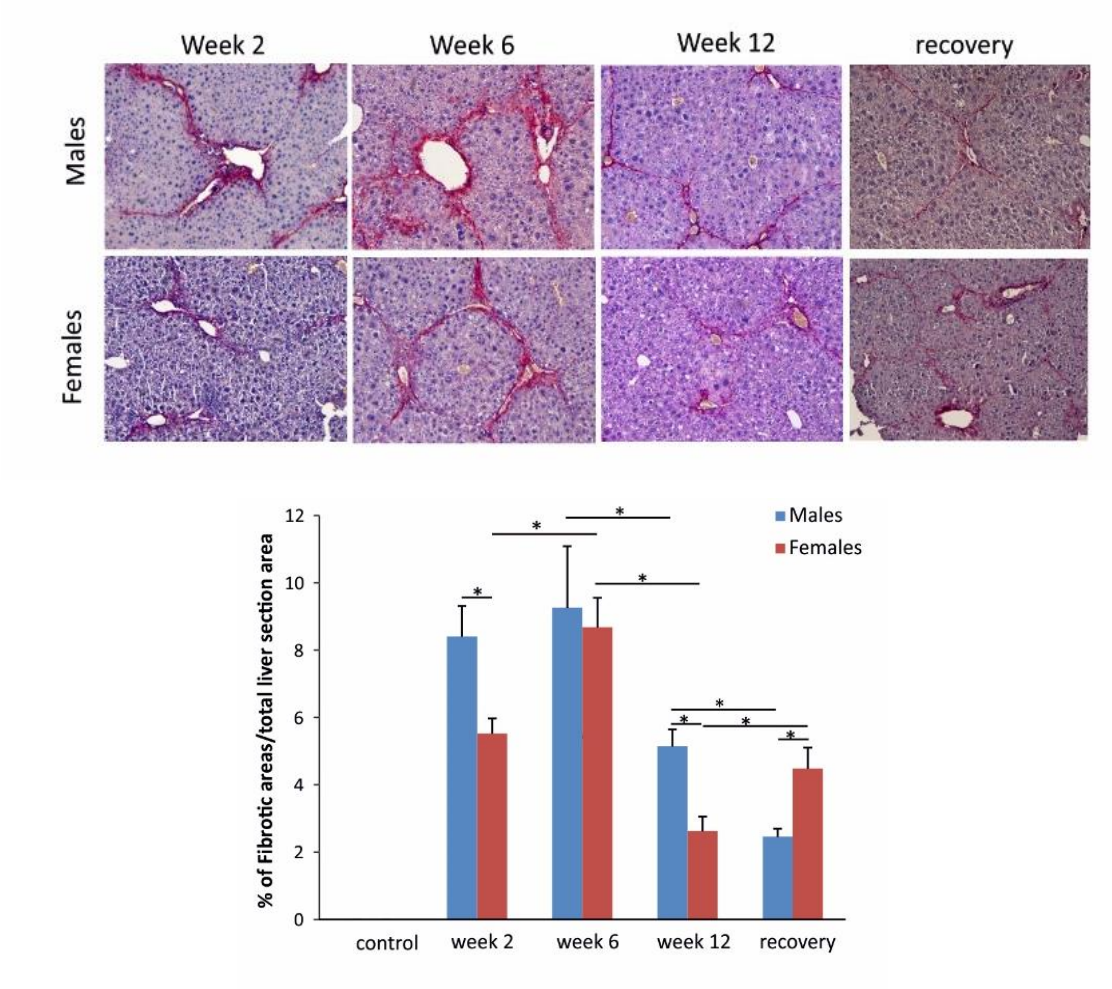

Figure 9. Analysis of fibrotic hepatic parenchyma by means of Sirius Red Staining. Top. Representative images (magnification 100x) of livers at week 2, 6, 12 and after the self-healing for either male or female mice are reported. Bottom. Fibrosis quantifications are reported. Data are expressed as mean±SE. *p<0.05.

HSCs activation

Alpha-SMA^{+} areas amount significantly differed between male and female animals at week 2 (males *vs* females: 5.47±0.88 *vs* 8.52±0.7 p=0.009), with an overall significant decrease over time within each gender (males at week 2 *vs* week 12 and females at week 2 *vs* week 12: 5.47±0.88 *vs* 1.58±0.68 p=0.004 and 8.52±0.7 *vs* 2.72±0.24 p<0.001, respectively) (Figure 10).

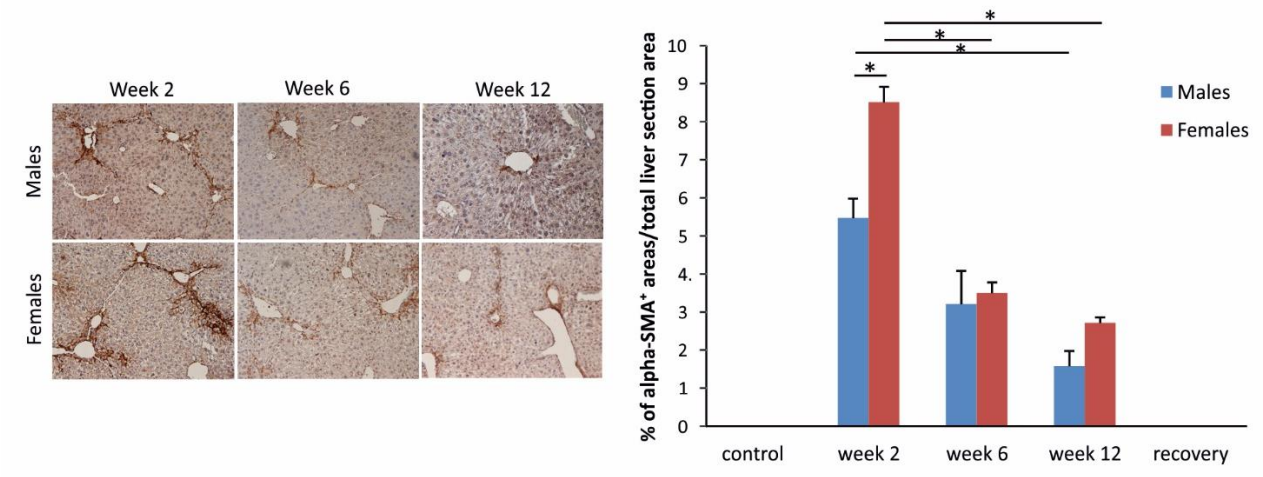

Figure 10. Analysis and quantification of activated HSCs by means of IHC for α-SMA immunoreactive areas. Representative images (magnification 100x) of livers at week 2, 6, 12 and after the self-healing for either male or female mice are reported on the left. Alpha-SMA quantifications are reported on the right. For α-SMA, immunoreactive sites from vascular regions were excluded. Data are expressed as mean±SE. *p<0.05.

CYP2E1 western blot analysis

The evaluation by western blot of the amount of CYP2E1 in males and females during a chronic liver damage revealed no gender-related differences at any time point, as summarized in Figure 11.

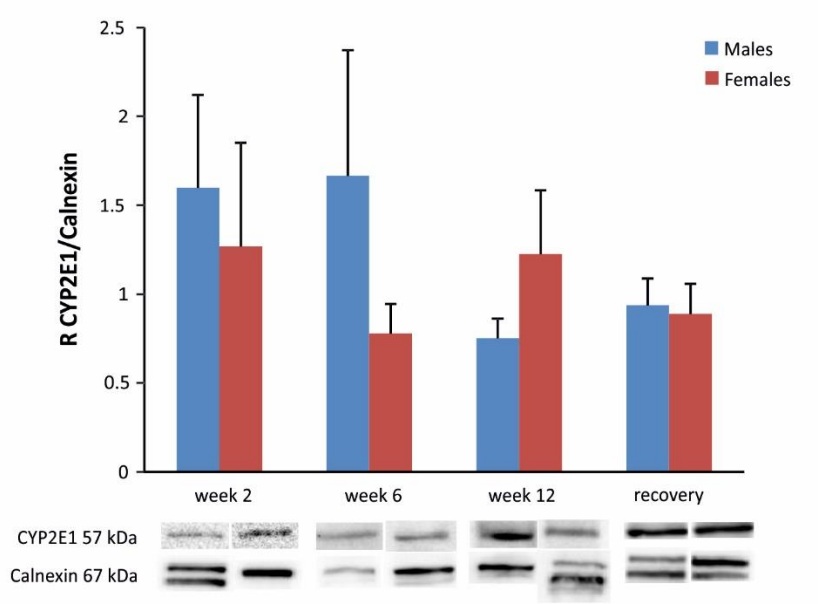

Figure 11. Western Blot analysis of CYP2E1 on total liver proteic lysates. The housekeeping used in this setting of experiments was calnexin. Data are expressed as R CYP2E1/Calnexin.

Collagens modulation

Collagen -I -III and -IV were analysed by Western Blot. Collagens were found higher in males than in females at week 2 (males *vs* females: 0.099±0.003 *vs* 0.003±0.0003 p=0.008 for collagen-I; 0.47±0.11 *vs* 0.1±0.01 p=0.008 for collagen–III; 0.21±0.018 *vs* 0.03±0.005 p=0.008 for collagen-IV).

The recovery group showed an opposite trend (males *vs* females: 0.086±0.01 *vs* 0.27±0.05 p=0.016 for collagen-I; 0.41±0.033 *vs* 0.74±0.09 p=0.016 for collagen–III; 0.14±0.03 *vs* 0.29±0.02 p=0.005 for collagen-IV) (Figure 12 and 13).

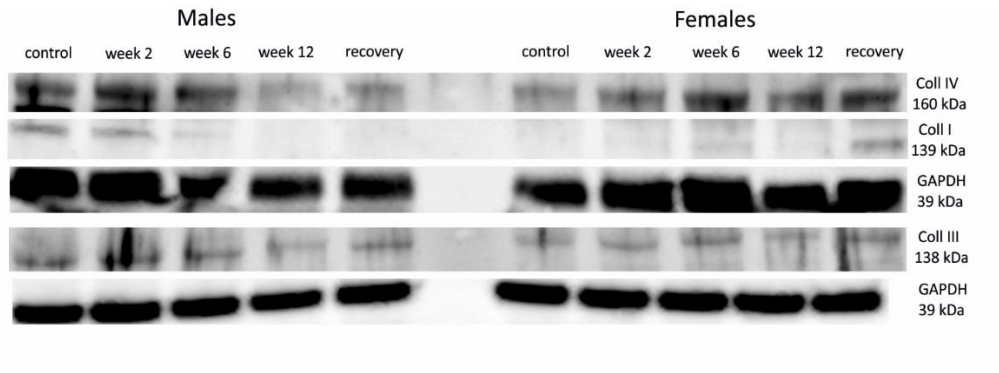

Figure 12. WB representative membranes for Collagen I, III and IV modulations, evaluated on total liver homogenates at different time frames of the chronic hepatic damage.

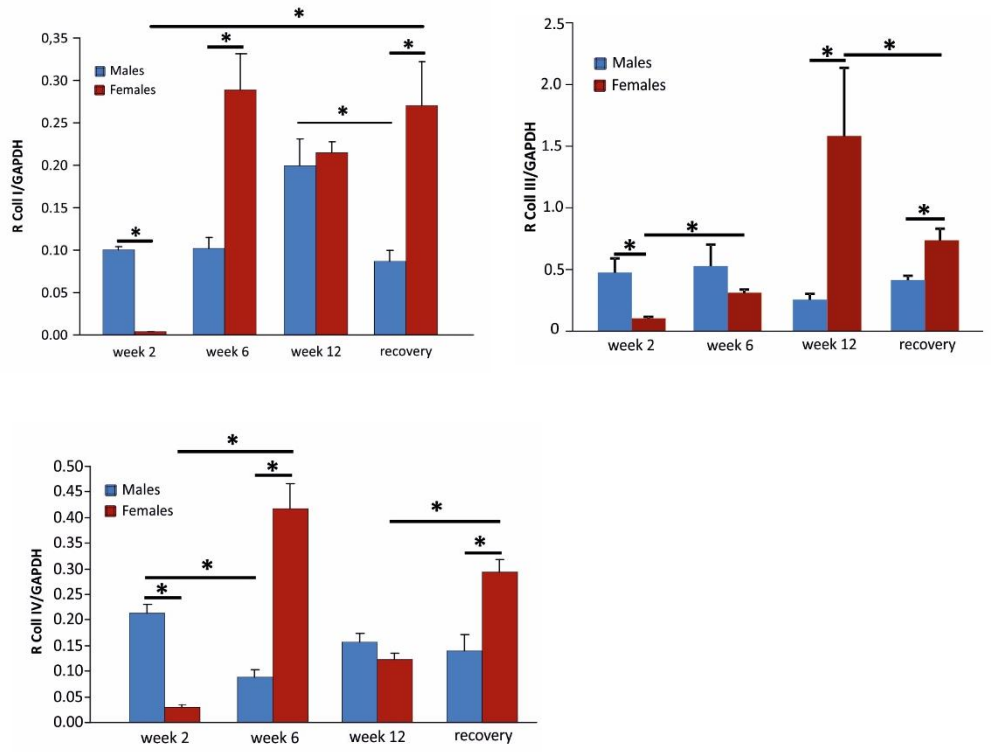

Figure 13. Quantification of the signals as R Collagen/GAPDH (right). Data are expressed as mean±SE. *p<0.05.

MMP9 activity and TIMP-1 protein regulation

MMP-9 activity was prominent in males in respect to females in the onset of the chronic insult -at week 2- (males *vs* females: 1.62±0.25 *vs* 1.05±0.17 p=0.026) (Figure 14). Moreover during the self-healing, male mice, differently from female mice, showed a significant decrease in the activity of

MMP-9 (males at week 12 *vs* recovery and females at week 12 *vs* recovery: 1.34±0.21 *vs* 0.54±0.15 p=0.02, and 0.54±0.18 *vs* 0.34±0.08 p=0.342, respectively) (Figure 14).

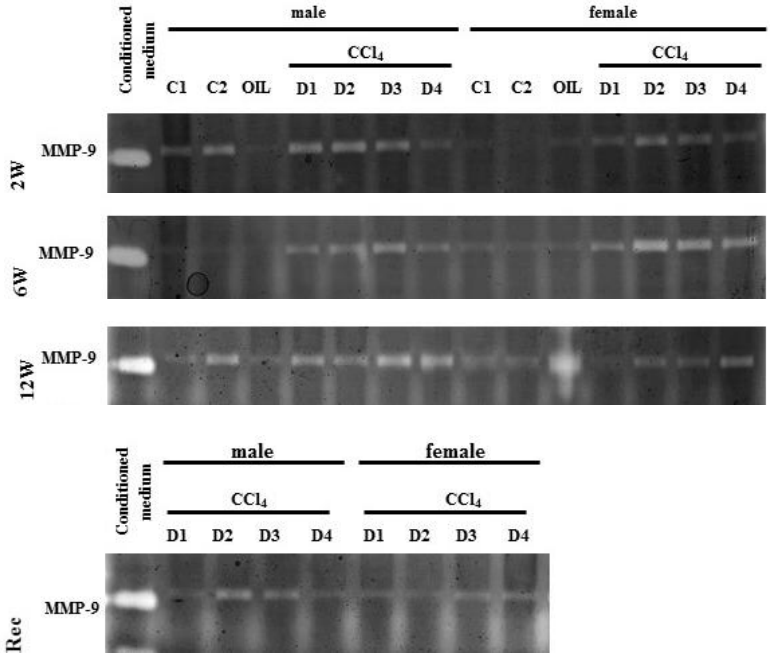

Figure 14. Quantification of the activity of MMP9, evaluated by means of zymography in control animals and in animals at various severity of hepatic injury. A representative image of zymography is reported below the quantification. Data are expressed as mean±SE * p<0.05.

TIMP-1 western blot analysis revealed an accumulation of the protein from week 2 to week 12 (p=0.016), solely in treated females. A statistically significant difference in the amount of the protein was apparent between treated male and female mice at the end of the treatment (males at week 12 *vs* females at week 12: 0.18±0.04 *vs* 4.65±1.27, p=0.016). Moreover, after the self-healing, TIMP-1 was found decreased (p=0.029) (Figure 15).

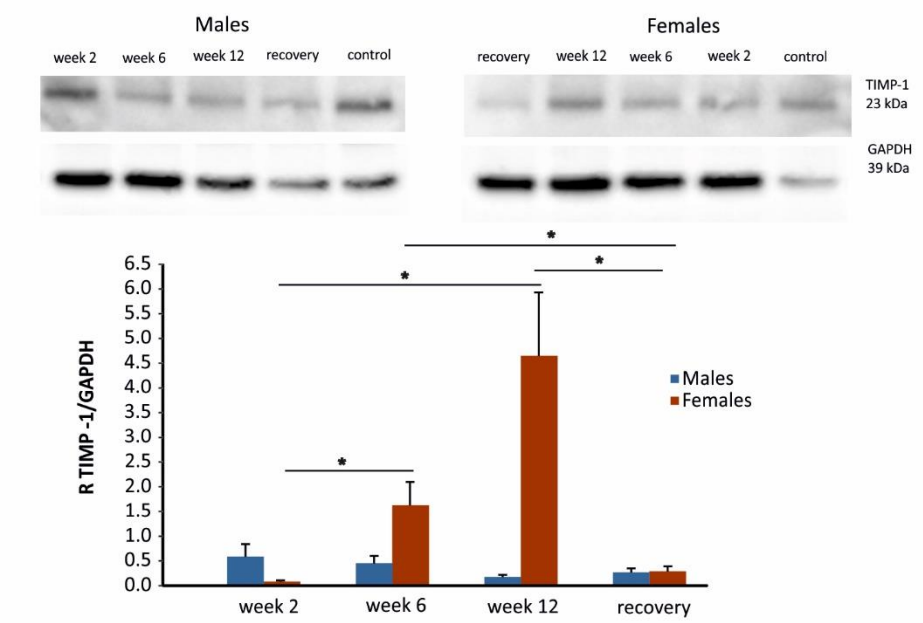

Figure 15. WB representative membranes for TIMP-1 modulations, evaluated on total liver homogenates at different time points of the chronic hepatic damage (top) and quantification of the signals as R Collagen/GAPDH (bottom). Data are expressed as mean±SE. *p<0.05.

Hepatocytes apoptosis evaluation

Apoptotic hepatocytes were evaluated by means of IHC for Asp-175. The amount of apoptosis was found higher in male in respect to female mice at week 2 (males *vs* females: 16.64±3 *vs* 9.14±4.4 p=0.03); the amount of Asp-175^{+} cells in both male and female mice significantly increased at week 12 (males week 2 *vs* week 12 and females at week 2 *vs* week 12: 16.64±3 *vs* 22.73±4.6 p=0.04 and 9.14±4.4 *vs* 24.09±4.7 p=0.008) and decreased from week 12 to the recovery period, to values comparable to those observed at the beginning of the treatment (females at week 12 *vs* recovery and males week 12 *vs* recovery: 24.09±4.7 *vs* 8.07±5.9 p=0.016 and 22.73±4.6 *vs* 15.1±5.12 p=0.0041) (Figure 16).

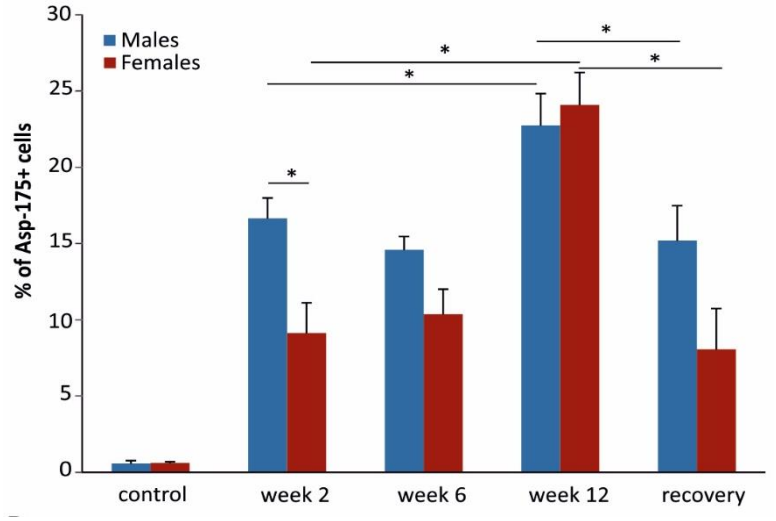
Males
Females
% of Asp-175+ cells
30
25
20
15
10
5
0
*
*
*
*
*
control
week 2
week 6
week 12
recovery

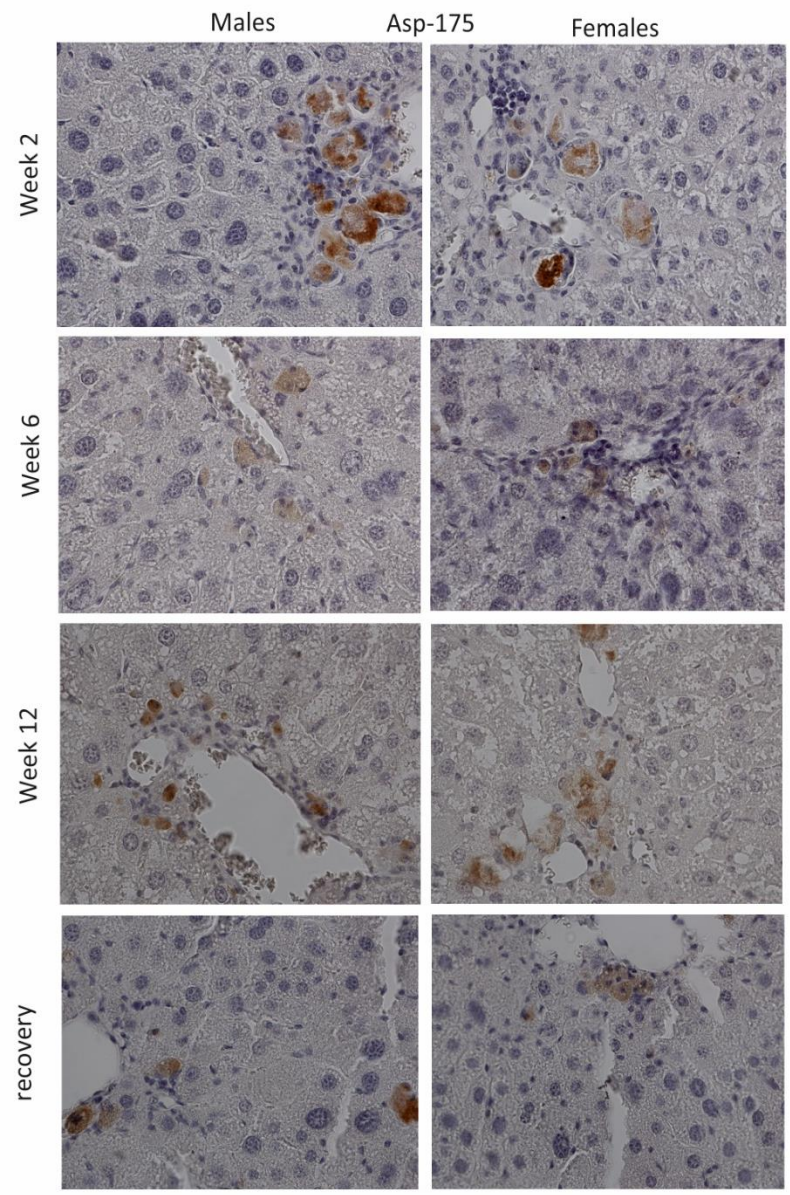
Males
Asp-175
Females
Week 2
Week 6
Week 12
recovery

Figure 16. Analysis of apoptosis of hepatocytes by means of IHC for Asp-175. Top. The histogram reported on the left represents the percentage of Asp-175$^+$ cells expressed as a mean±SE of the values calculated for each slide for each experimental group. Bottom. Representative images of week 2, 6, 12, and recovery are shown on the right. HPF magnification 400x. *p<0.05.

MMP9 mRNA modulation

The molecular modulations of MMP9 mRNA were evaluated. The real-time PCR analysis revealed a significant down modulation of about 68% (p=0.008) in males from week 6 to the end of the recovery period; moreover MMP9 mRNA was found higher (150%) in females than in males of the recovery group (p=0.008) (Figure 17).

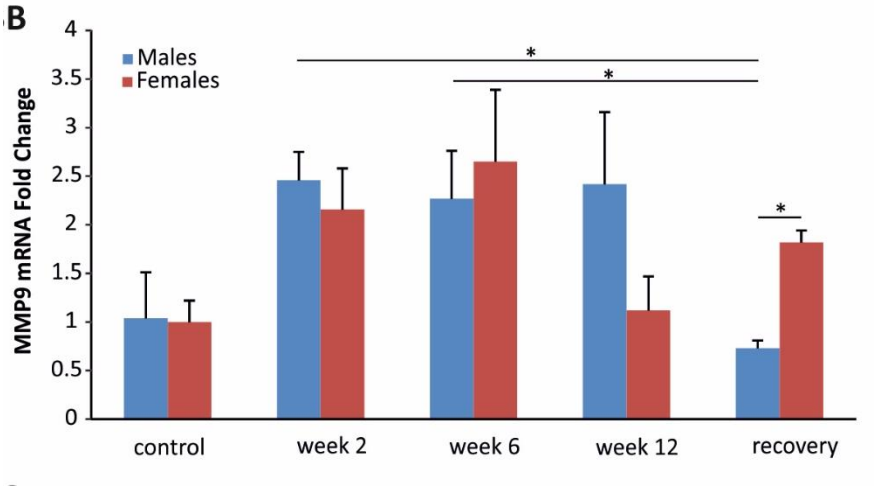

Figure 17. Evaluation of MMP9 mRNA modulation during chronic hepatic damage on total liver homogenates. Results were normalized to those of mRNA encoding GAPDH (calculated by the change-in-cycling-threshold method as $2^{-\Delta\Delta C(t)}$ and are presented relative to those of control male mice, set as 1. Data are presented as mean±SE. * p<0.05.

IHC evaluation of F4/80$^+$ and CK7$^+$ cells

To evaluate the amount of activated macrophages in the hepatic parenchyma, an IHC for F4/80 was performed. As evidenced in Figure 18, at week 2 the amount of positive cells was higher in males than in females (males *vs* females 10.27±1.62 *vs* 3.88±0.46 p=0.016). An overall decrease in the percent of F4/80$^+$ cells after the self-healing from the chronic hepatic damage was apparent in treated males (males at week 2 *vs* males in the recovery 10.27±1.62 *vs* 3.88±0.46 p=0.016). On the contrary the number of activated macrophages significantly increased in treated females in the same time frame (males at week 2 *vs* males in the recovery 3.87±0.64 *vs* 5.87±0.64 p=0.016). Interestingly, treated males after the self-healing showed a significant decrease in the percentage of activated macrophages (males at week 12 *vs* males in the recovery 7.91±1.14 *vs* 4.5±0.7 p=0.031).

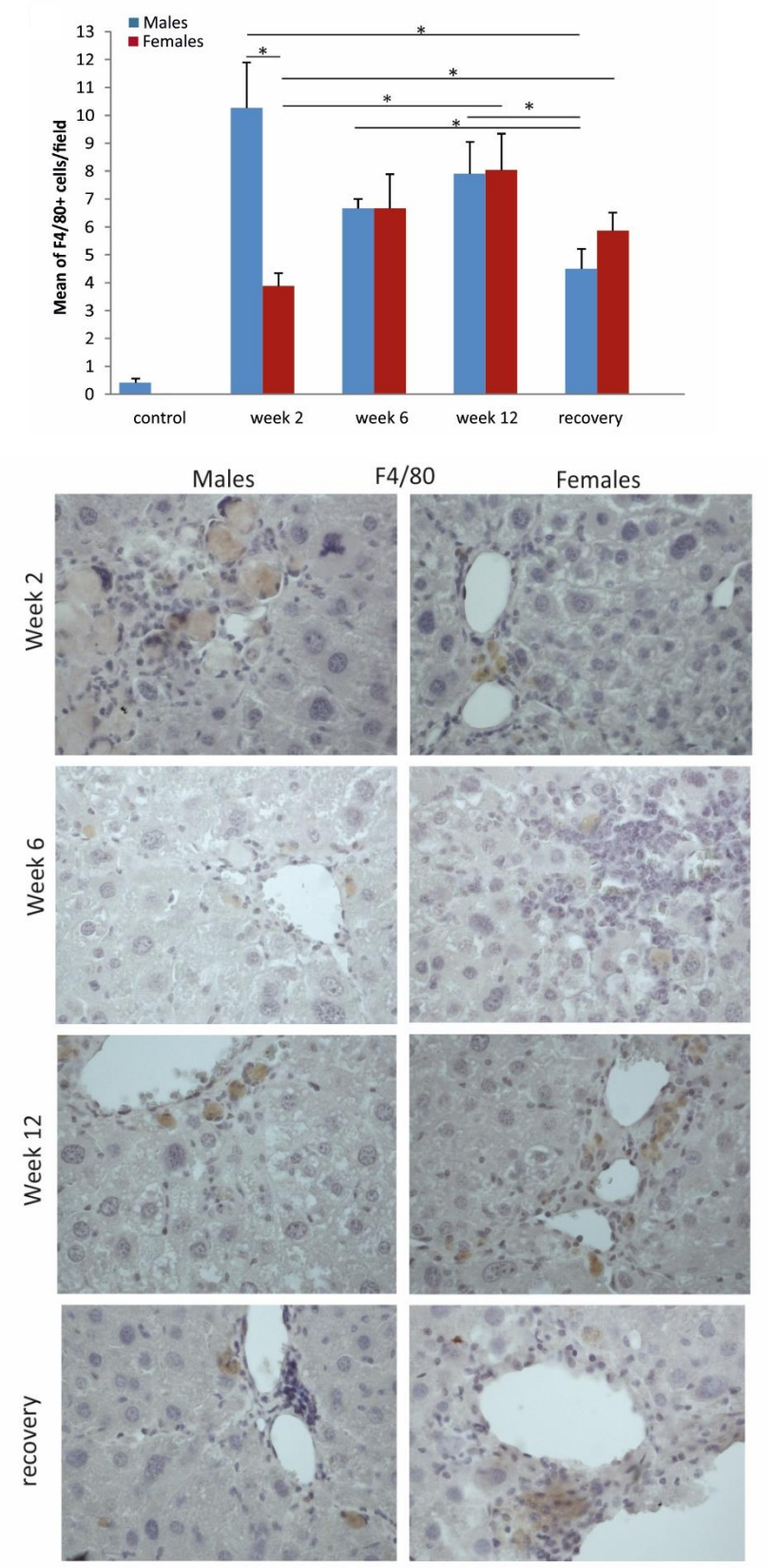

Figure 18. Evaluation of activated macrophages in the parenchyma of injured livers by means of IHC for F4/80. Top. The histogram represents the percentage of F4/80^{+} cells expressed as a mean±SE of the values calculated for each slide

for each experimental group Bottom. Representative images at different time point are reported. HPF magnification 400x. *p<0.05.

Data on CK7^{+} cells, as an index of progenitor cell/biliary phenotype, are presented in Figure 19. The percentage of CK7^{+} cells significantly decreased from week 2 to recovery both in treated males and females (males at week 2 *vs* males in the recovery and females at week 2 *vs* females in the recovery: 12.8±3.52 *vs* 6±0.96 p=0.003 and 17.12±6.09 *vs* 7.64±2.5 p=0.012, respectively).

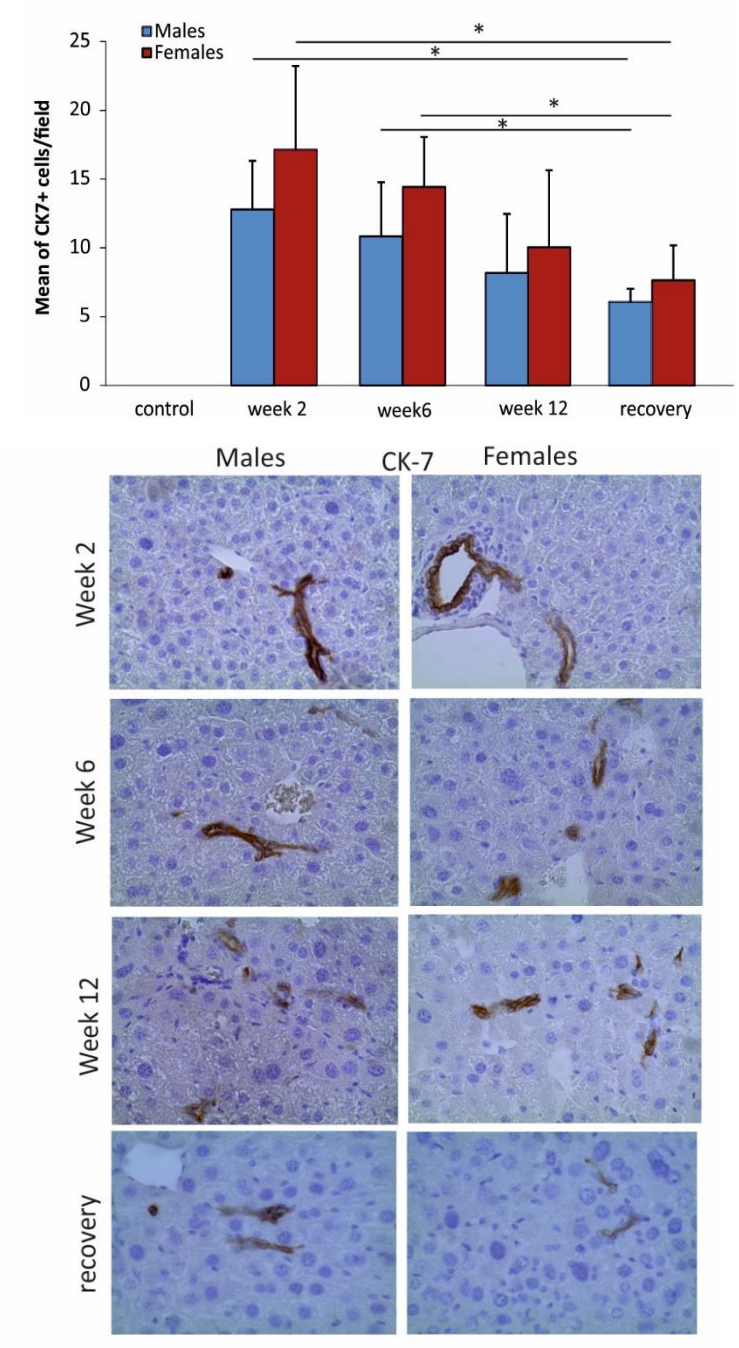

Figure 19. IHC for CK-7 as an index of progenitor cell/biliary phenotype. Top. The histogram represents the percentage of $CK7^+$ cells expressed as a mean±SE of the values calculated for each slide for each experimental group. Bottom. Representative images at different time point are reported. HPF magnification 400x. *p<0.05.

VEGFA protein and mRNA regulation

Analysis of VEGFA protein modulation revealed that the protein was lower in female in respect to male mice at week 12 (males *vs* females: 1.38±0.09 *vs* 0.62±0.08 p<0.001). The protein was observed to dramatically increase during the recovery period in both (males at week 12 *vs* recovery and females at week 12 *vs* recovery: 1.38±0.09 *vs* 5.9±0.6 p=0.008 and 0.62±0.08 *vs* 6.9±1.16 p=0.008, respectively) (Figure 20).

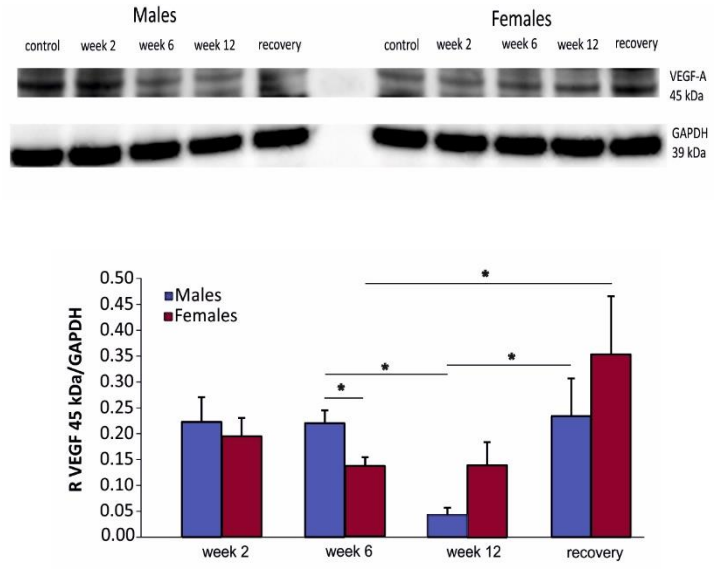

Figure 20. WB for VEGFA evaluated on total liver homogenates at different time points of the chronic hepatic damage. A representative membrane (top) and the quantification of the signals as mean±SE of R VEGF-A/GAPDH (bottom) are reported. Data are expressed as mean±SE. *p<0.05.

If considering VEGFA mRNA modulations, it was apparent that CCl_4 intoxication determines an overall down-modulation of VEGFA mRNA in respect to control animals, most prominent in treated male mice. Significant differences in VEGFA mRNA levels between males and females were observed both at week 2 and 6. Interestingly, VEGFA mRNA was significantly upregulated in females at week 2 of about 90% (p=0.016) while at week 6 it was down-regulated of about 50% (p=0.008), in respect to males. A progressive and significant increase in VEGFA mRNA was observed in females from week 6 to the end of the self-healing period (p=0.008), with an overall upregulation of mRNA of about 140%. The situation was different in male mice, in which the mRNA of VEGFA significantly decreased of about 42% from week 6 to week 12 (p=0.008) and it was found up-regulated of about 66% from week 12 to recovery (p=0.016) (Figure 21).

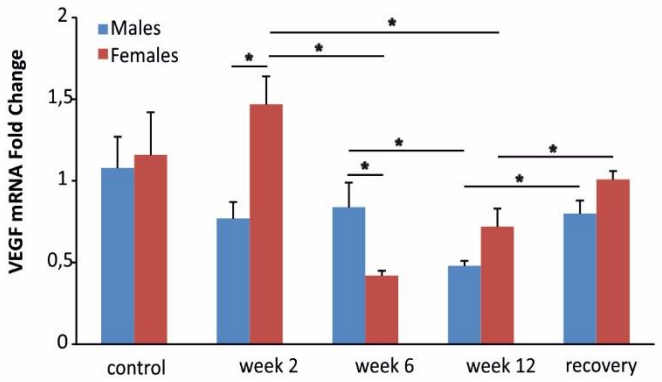

Figure 21. Real time PCR for VEGFA mRNA performed on total liver homogenates. Results were normalized to those of mRNA encoding GAPDH (calculated by the change-in-cycling-threshold method as $2^{-\Delta\Delta C(t)}$) and are presented relative to those of control male mice, set as 1. Data are presented as mean±SE. *p<0.05.

IL-6 protein and mRNA modulations

Western Blot analysis on IL-6 showed that the protein was found lower in females at week 2 in respect to males (males *vs* females: 0.28±0.02 *vs* 0.033±0.004 p=0.008). Interestingly, male mice, differently from female mice, showed a significant decrease in the amount of IL-6 from week 6 to week 12 (males at week 6 *vs* week 12 and females at week 6 *vs* week 12: 3.2±1.3 *vs* 0.42±0.06 p=0.008 and 1.11±0.17 *vs* 0.7±0.26 p=0.3 respectively). Moreover male mice showed a significant increase of IL-6, after the cessation of CCl_4 intoxication and during the recovery period, differently from female mice (males at week 12 *vs* recovery and females at week 12 *vs* recovery: 0.42±0.06 *vs* 2.4±0.28 p=0.008 and 0.7±0.26 *vs* 1.88±0.41 p=0.06, respectively) (Figure 22).

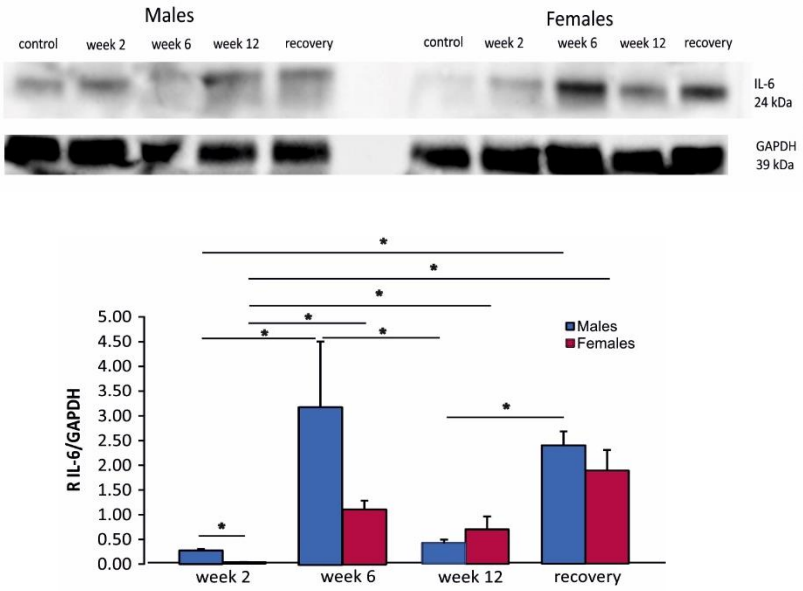

Figure 22. WB for IL-6 evaluated on total liver homogenates at different time points of the chronic hepatic damage. Top. A representative membrane is reported. Bottom. Quantification of the signals as mean±SE of R IL-6/GAPDH (right) is reported. Data are expressed as mean±SE. *p<0.05.

IL-6 mRNA significantly increased in treated male mice along the chronic hepatic damage (males at week 2 *vs* males at week 12: 0.65±0.14 *vs* 1.69±0.31 p=0.022). When male mice were allowed to self-heal, IL-6 mRNA was observed to significantly decrease of about 60% (males at week 12 *vs* males recovery: 1.69±0.31 *vs* 0.68±0.11 p=0.012). Moreover IL-6 mRNA was significantly down-modulated in females in respect to males both at week 6 and in the recovery group of about 64% and 57%, respectively (Figure 23).

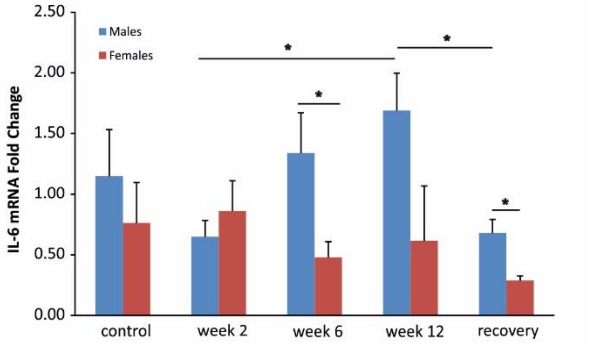

Figure 23. Real time PCR for IL-6 mRNA performed on total liver homogenates. Results were normalized to those of mRNA encoding GAPDH (calculated by the change-in-cycling-threshold method as $2^{-\Delta\Delta C(t)}$) and are presented relative to those of control male mice, set as 1. Data are presented as mean±SE. *p<0.05.

Evaluation of Macrophages-associated transcripts

MMP13 mRNA real-time PCR analysis revealed a progressive down modulation of MMP13 mRNA in females from week 6 to the end of the recovery period of about 72% (p=0.032) with a significant difference in MMP13 mRNA between females and males at week 12 (males *vs* females: 3±0.4 *vs* 1.09±0.14 p=0.016) (Figure 24).

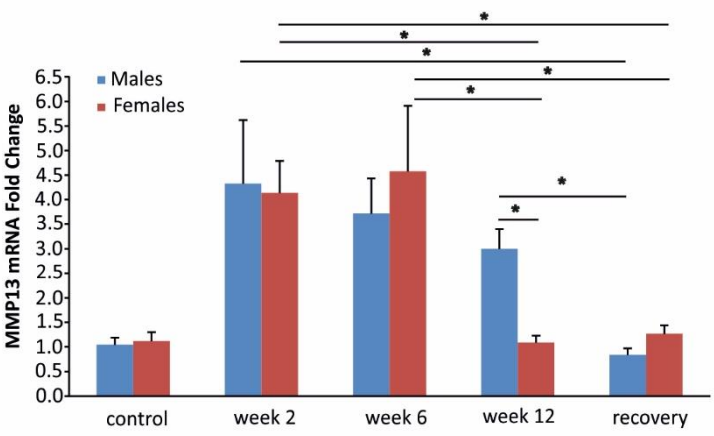

Figure 24. Real time PCR for MMP13 mRNA performed on total liver homogenates. Results were normalized to those of mRNA encoding GAPDH (calculated by the change-in-cycling-threshold method as $2^{-\Delta\Delta C(t)}$) and are presented relative to those of control male mice, set as 1. Data are presented as mean±SE. *p<0.05.

IL-12β mRNA showed an overall significant decrease in treated females from week 2 to week 12 (females at week 2 *vs* females at week 12: 4.54±1.02 *vs* 1.05±0.24 p=0.036) and interestingly, if considering the period between week 6 and the recovery, IL-12β mRNA in treated female was significantly upregulated (females at week 6 *vs* females at recovery: 3.12±0.64 *vs* 7.15±1.31 p=0.032). IL-12β mRNA of females was significantly upregulated in respect to males both at week 2 and in the recovery group of about 128% (p=0.034) and 133% (p=0.032), respectively (Figure 25).

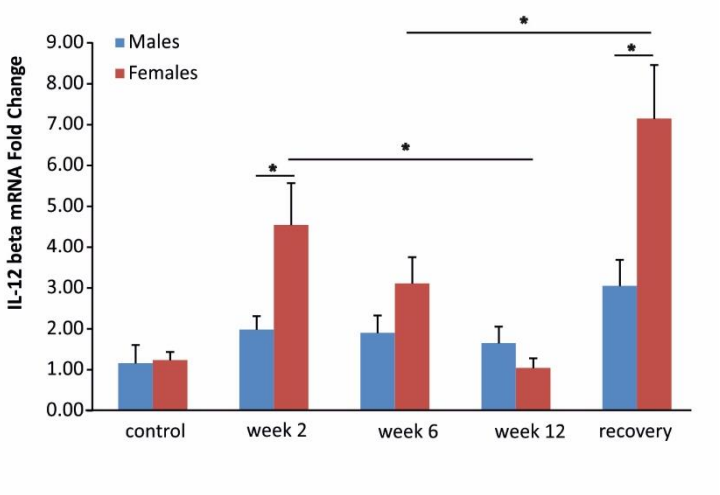

Figure 25. Real time PCR for IL-12 beta mRNA performed on total liver homogenates. Results were normalized to those of mRNA encoding GAPDH (calculated by the change-in-cycling-threshold method as $2^{-\Delta\Delta C(t)}$) and are presented relative to those of control male mice, set as 1. Data are presented as mean±SE. *p<0.05.

CXCL9 mRNA of females was significantly upregulated in respect to males both in the control, at week 2 and in the recovery group of about 577% (p=0.017), 129% (p=0.016) and 167% (p=0.008), respectively (Figure 26). Moreover CXCL9 mRNA increased in treated males from week 2 to week 12 (males at week 2 *vs* males at week 12: 1.38±0.13 *vs* 2.6±0.4 p=0.032), and decreased after the self-healing (males at week 12 *vs* males at recovery: 2.6±0.4 *vs* 1.16±0.22 p=0.008).

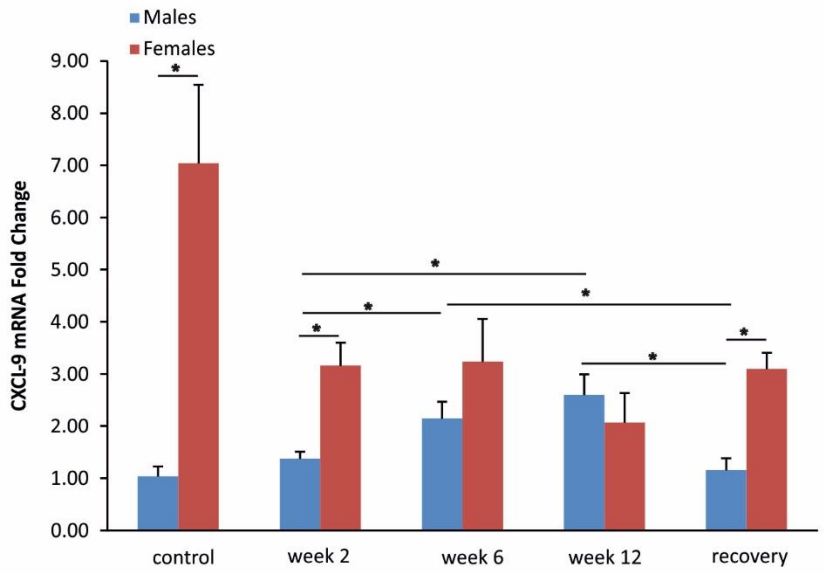

Figure 26. Real time PCR for CXCL9 mRNA performed on total liver homogenates. Results were normalized to those of mRNA encoding GAPDH (calculated by the change-in-cycling-threshold method as $2^{-\Delta\Delta C(t)}$) and are presented relative to those of control male mice, set as 1. Data are presented as mean±SE. *p<0.05.

FCM Analysis of the hepatic inflammatory infiltrate

In the evaluation of the immune populations infiltrating the injured hepatic parenchyma, Kupffer cells, dendritic cells and a population of restorative macrophages were considered. Kupffer cells population, defined as $CD11b^+F4/80^+$, from week 2 across the self-healing, showed an overall decrease in the % for both treated males and females (males at week 2 *vs* males at recovery: 4.39±1.29 *vs* 0.16±0.11 p=0.008; females at week 2 *vs* females at recovery: 8.52±2.91 *vs* 1.03±0.34 p=0.008). Moreover recovery groups significantly differed in the amount of this cell population (males at recovery *vs* females at recovery: 0.16±0.11 *vs* 1.03±0.34p=0.016) (Figure 27 top).

Dendritic cells ($CD11b^+CD11c^+$) infiltration represented an early event in the establishment of chronic liver damage (Figure 27 middle). An overall decrease in their amount was observed both in treated males and females from week 2 to week 12 (males at week 2 *vs* males at week 12: 12.65±4 *vs* 0.57±0.04 p=0.0018; females at week 2 *vs* females at week 12: 22.8±7.15 *vs* 1.32±0.44 p=0.008) and also from week 2 to the self-healing period (males at week 2 *vs* males at recovery: 12.65±4 *vs* 1.22±0.42 p=0.024; females at week 2 *vs* females at recovery: 22.8±7.15 *vs* 1.14±0.24 p=0.008).

$F4/80^+GATA6^+$ macrophages were evaluated on both $CD45^+$ and $CD45^-$ gates. As evidenced in Fig. 6C, this population infiltrated at very low levels both control female and male mice liver with a trend to be higher in females at week 2 in respect to males. A reversion in its abundance in the recovery group was observed (recovery males *vs* recovery females: 1.08±0.6 *vs* 0.1±0.06 p=0.029). Moreover a significant increase in $GATA6^+$ macrophages was observed in males from week 2 to the recovery (males a week 2 *vs* recovery: 0.1±0.05 *vs* 1.08±0.6 p=0.029) (Figure 27 bottom).

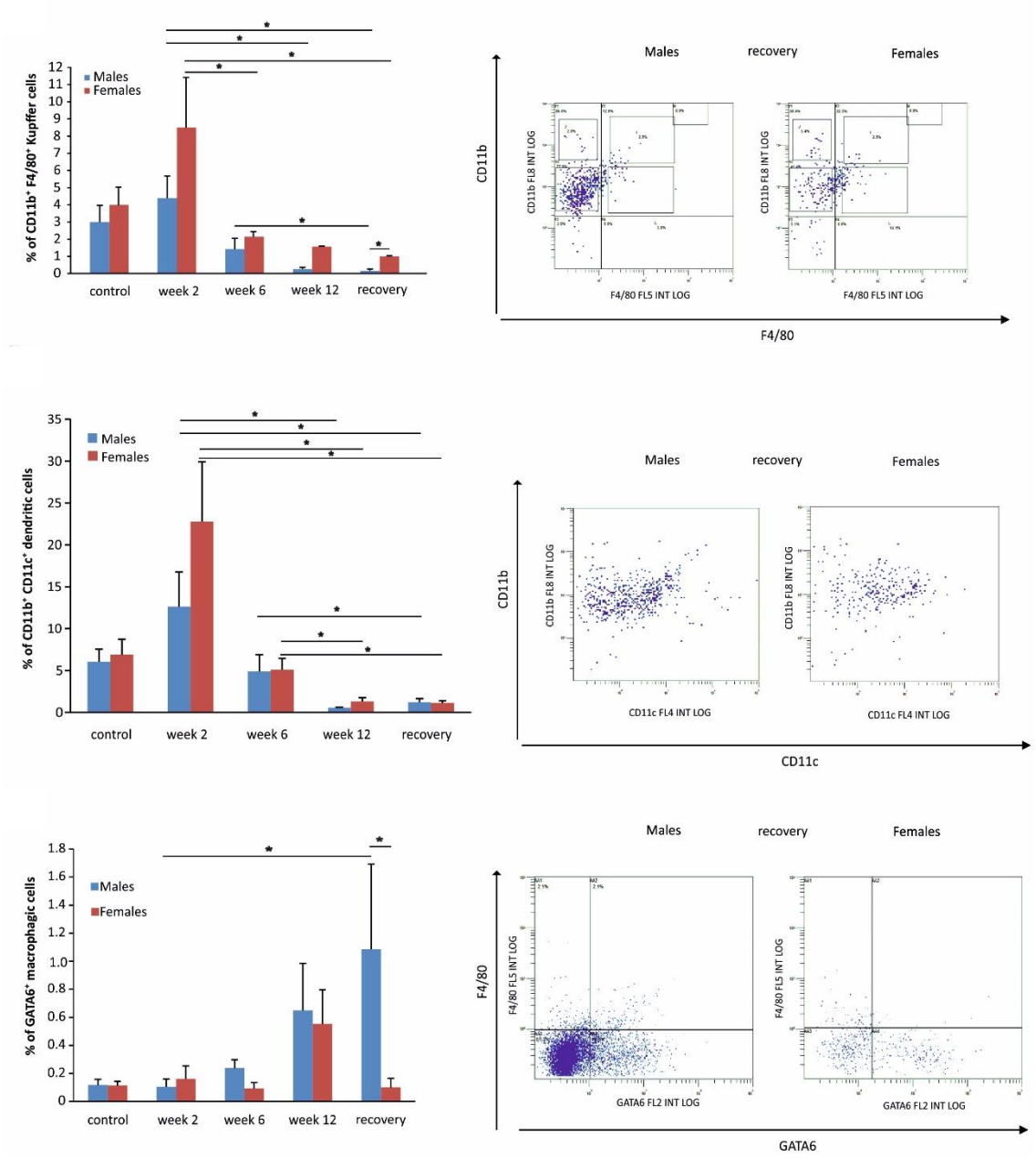

Figure 27. Flow cytometric characterization of injured liver immune cell populations. Top. Kupffer cells (double positive $CD11b^+F4/80^+$ cells) evaluation in single cell suspensions of livers of animals (controls and at different timeframes of hepatic damage) was performed as follows: 30000 events were acquired; the number of events related to $CD45^+$/tot events was calculated as % of $CD45^+$x30000 events/100 [named C]; then the number of events related to double $CD11b^+$ and $F4/80^+$/tot events was calculated as % of $CD11b^+F4/80^+$x C/100 [named D]; finally Dx100/30000 events was the % of $CD11b^+F4/80^+$ related to the total (and this value was reported). *$p<0.05$. Middle. Dendritic cells (double positive $CD11b^+CD11c^+$) evaluation in single cell suspensions of livers of animals (controls and at different time-points of hepatic damage) was performed as follows: 30000 events were acquired; the number of events related to $CD45^+$/tot events was calculated as % of $CD45^+$x30000 events/100 [named C]; then the number of events related to double $CD11b^+$ and $CD11c^+$/tot events was calculated as % of $CD11b^+CD11c^+$x C/100 [named D]; finally Dx100/30000 events was the % of

$CD11b^+CD11c^+$ related to the total (and this value was reported). *p<0.05. Bottom. Double positive $F4/80^+GATA6^+$ macrophages (gated on both $CD45^+$ and $CD45^-$) evaluation in single cell suspensions of livers of animals (controls and at different time-points of hepatic damage) was performed as follows: 30000 events were acquired; the number of events related to $CD45^+$/tot events was calculated as % of $CD45^+$x30000 events/100 [named C]; then the number of events related to double $F4/80^+$ and $GATA6^+$/tot events was calculated as % of $F4/80^+GATA6^+$x C/100 [named D]; finally Dx100/30000 events was the % of $F4/80^+GATA6^+$ related to the total of $CD45^+$ cells [named E]. The same approach was applied for $CD45^-$[named F]. The sum of E+F resulted in the % of $F4/80^+GATA6^+$ related to the total of $CD45^+$and $CD45^-$ gates (and this value was reported). *p<0.05.

Serum cytokines flows

In Figure 28 data regarding the sera measurements of a panel of cytokines are reported. More in detail serum measurement of GM-CSF (pg/mL) showed that a significant difference between control males and females existed (control males *vs* control females: 68.71±13.72 *vs* 26.2±2.71 p=0.023). GM-CSF was higher in treated females in respect to treated males at week 2 (males at week 2 *vs* females at week 2: 37.25±7.06 *vs* 77±9.4 p=0.029). It significantly decreased both in males and females from week 2 to week 12, with the course most pronounced in the latter (males at week 2 *vs* males at week 12: 37.25±7.06 *vs* 10.24±1.93 p=0.025; females at week 2 *vs* females at week 12: 77±9.4 *vs* 40.13±8.42 p=0.038). Interestingly, an increase in the amount of GM-CSF was observed in treated males during the self-healing (males at week 12 *vs* males at recovery: 10.24±1.93 *vs* 29.04±5.47 p=0.037).

IFN-gamma (pg/mL) showed significant fluctuations exclusively in treated males. In particular it was found decreased from week 2 to week 6 (males at week 2 *vs* males at week 6 643.2±169.74 *vs* 238.98±59.3 p=0.016), thus showing an increasing trend during the self-healing (males at week 12 *vs* males at recovery: 78.53±29.4 *vs* 241.83±27.67 p=0.03).

IL-1 alpha (pg/mL) was not significantly modulated between treated males and females during the chronic injury.

IL-1 beta (pg/mL) levels were found significantly higher in treated females than in males both at week 6 and 12 (males at week 6 *vs* females at week 6: 34.87±0.001 *vs* 60.6±13.4 p=0.029; males at week 12 *vs* females at week 12: 0 *vs* 22.5±0.001 p=0.036). It significantly decreased in both from week 2 to week 12 (males at week 2 *vs* males at week 12: 85.74±10.54 *vs* 0 p=0.036; females at week 2 *vs* females at week 12: 103.97±11.95 *vs* 22.5±0.001 p=0.036). Interestingly IL-1 beta increased in males during the recovery (males at week 12 *vs* males at recovery: 0 *vs* 59.73±5.99 p=0.016).

IL-2 (pg/mL) significantly differed in its levels in control animals (control males *vs* control females: 54.51±5.94 *vs* 30.12±5.67 p=0.041). The levels of IL-2 were found higher in females in respect to males both at week 2 and 12 (males at week 2 *vs* females at week 2: 21.25±3.44 *vs* 54.08±5.6 p=0.016;

males at week 12 *vs* females at week 12: 5.46±1.25 *vs* 20.63±2.53 p=0.002). A significant decrease of the cytokine was observed in both from week 2 to week 12 (males at week 2 *vs* males at week 12: 21.25±3.44 *vs* 5.46±1.25 p=0.016; females at week 2 *vs* females at week 12: 54.08±565 *vs* 20.63±2.53 p=0.005). Interestingly, treated males, when allowed to self-heal, showed a significant increase in IL-2 (males at week 12 *vs* males at recovery: 5.46±1.25 *vs* 19.36±3.4 p=0.029).

IL-4 (pg/mL) was found higher in males in respect to females at week 2 (males at week 2 *vs* females at week 2: 6.4±0.01 *vs* 3±0.36 p<0.001) (data not shown). IL-5 (pg/mL) was not measurable in males both at week 12 (males at week 12 *vs* females at week 12: 0 *vs* 19.14±0.31 p=0.036) and after the self-healing (here the cytokine was absent also in treated females) (data not shown). Serum IL-6 (pg/mL) was significantly higher in treated males, if compared to females at week 2 (males at week 2 *vs* females at week 2: 1998.13±650.64 *vs* 250.32±68.82 p=0.025). An overall decrease was apparent in treated males during the chronic liver damage (IL-6 was not measurable in males at week 12). After the self-healing the cytokine was below the LOD in both (data not shown). IL-9 was undetectable in controls animals. It significantly decreased in males from week 2 to week 6 (males at week 2 *vs* males at week 6: 64.2±8.4 *vs* 0 p<0.001) and of course, a significant difference was found between treated males and females at week 6 (males at week 6 *vs* females at week 6: 0 *vs* 23.95±4.36 p=0.005) (data not shown). IL-12 p70 significantly increased from week 6 to week 12 solely in treated females (females at week 6 *vs* females at week 12: 71.7±0.01 *vs* 129.24±0.01 p<0.001). Moreover it differed between treated males and females at week 12 (males at week 12 *vs* females at week 12: 0 *vs* 129.24±0.01 p=0.036) (data not shown). IL-17 (pg/mL) was almost undetectable or present at very low levels in treated males (mean±SE 3.09±1.06). A significant difference was observed between treated males and females at week 2 (; males at week 2 *vs* females at week 2: 2.22±1.02 *vs* 39.7±5.11 p<0.001). Furthermore IL-17 significantly decreased from week 2 to week 6 in treated females (females at week 2 *vs* females at week 6: 39.7±5.11 *vs* 20.75±0.01 p=0.003) (data not shown). MCP-1 (pg/mL) did not significantly differed between treated animals both at week 2 (males at week 2 *vs* females at week 2: 110.5±34.7 *vs* 79.3±26 p=0.55), although it became undetectable both at week 12 and in the recovery group in both (data not shown). M-CSF (pg/mL) was undetectable in control males, in treated females at week 2, in both at week 12 and in the recovery. At week 2 M-CSF was significantly higher in treated males than in females (males at week 2 *vs* females at week 2: 4.88±3.7 *vs* 0 p=0.036). Interestingly it showed a significant increase in treated females from week 2 to week 6 (females at week 2 *vs* females at week 6: 0 *vs* 5.08±2.15 p=0.036) (data not shown). Rantes (pg/mL) resulted below the LOD in treated males at week 12 and both in treated males and females after the self-healing. Interestingly the basal levels of the chemokine differed between control males and

females (control males *vs* control females: 11.88±5.14 *vs* 27.35±3.15 p=0.042) (data not shown). TNF-alpha (pg/mL) was measurable in treated males at week 2 (mean±SE 24.3±2.1) and in treated females at week 6 (mean±SE 46.89±0.01) (data not shown). As evidenced in Fig. 7, VEGFA was found significantly decreased in treated males from week 2 to week 6 (males at week 2 *vs* males at week 6: 97±14.1 *vs* 29.7±4.63 p=0.029), being almost invariable in the sera of treated females, and undetectable after the self-healing (Figure 28).

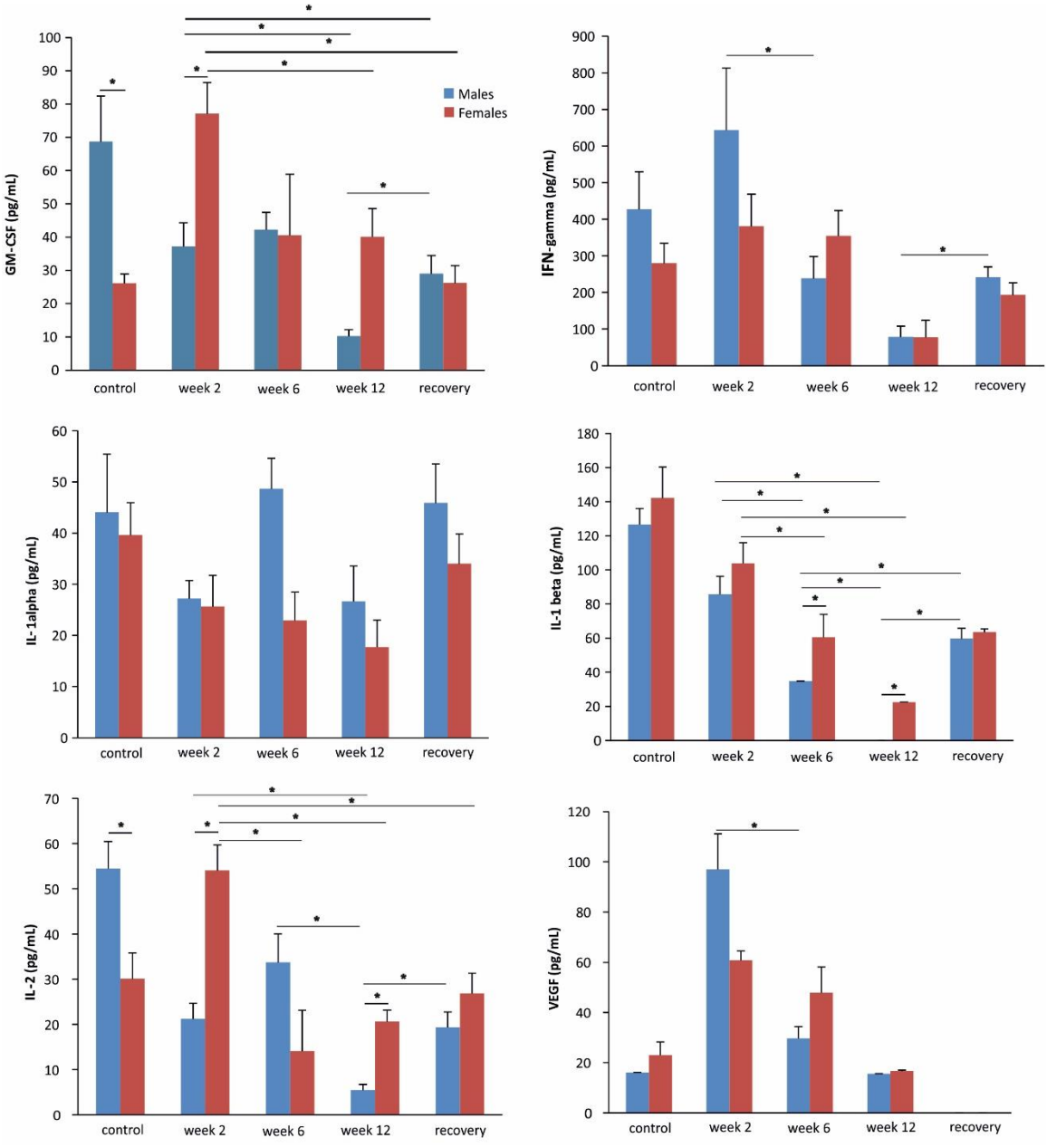

Figure 28. The circulating inflammatory profile of cytokines in males and females with a chronic hepatic damage. Most relevant data derived from multi-cytokines array analysis performed on a chip device with two-fold diluted sera of animals without or with a chronic hepatic damage at various grades of severity are reported. Data are presented as mean±SE. *p<0.05.

Measurement of serum estradiol and testosterone

As presented in Figure 29, estradiol (pg/mL) and testosterone (ng/dL) were evaluated in sera of animals treated or not with CCl_4. Estradiol differed in control animals (control males *vs* control females: 4.12±0.12 *vs* 8.07±1.67 p=0.018). It was interesting to analyse in females the time trend of the hormone during the chronic hepatic damage and after the self-healing (although any significance was reached). The differences between females and males in its concentrations were left. Testosterone was below the LOD in females. It showed fluctuations in treated males across the chronic hepatic damage, even though no statistical differences were observed (Figure 29).

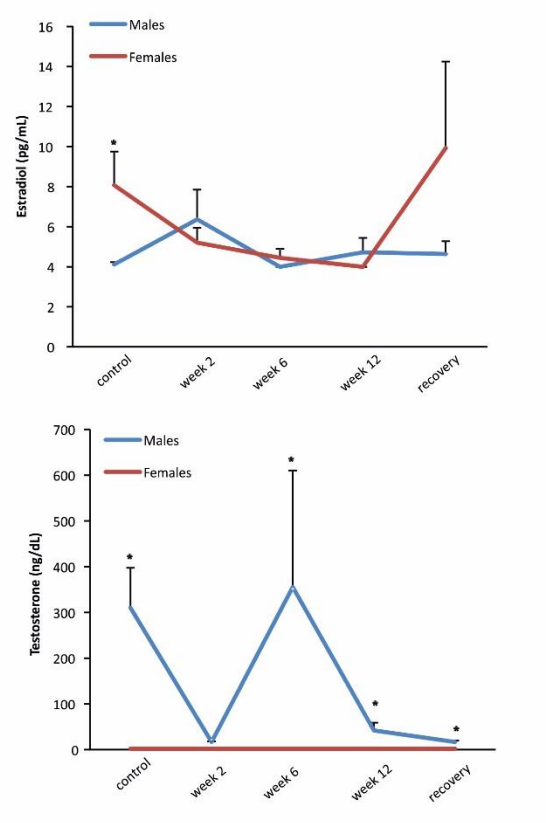

Figure 29. Estradiol (pg/mL) and Testosterone (ng/dL) serum evaluation in animals with different grading of chronic hepatic injury. Testosterone serum levels in female mice were always under limit of detection of the method (2.5 ng/dL). An arbitrary value of 2.4 was attributed to figure the trend. Data are presented as mean±SE. *p<0.05.

Discussion

Liver fibrosis is the result of an iterative insult and it represents a complex pathological process in which multiple components including KCs, HSCs, hepatocytes, and various cytokines and fibrotic matrix proteins are actively participating. Currently, extensive studies focus on establishing a mechanistic link between hepatocellular apoptosis, inflammation, and fibrosis in chronic liver diseases. Moreover on the basis of previous studies of our group in a murine model of an acute liver damage, also gender-related immune infiltrating populations proved to be a key determinant in the process of liver restoration. Translating these observations in a chronic setting of hepatic damage, with this PhD thesis research work we aimed at ascertaining to what extent being males or females influenced the biological processes of fibrosis resorption and liver regeneration.

After the development of a chronic damage in the liver of mice, by means of CCl_4 injection (Figure 6-7-8), the early activation of HSCs component was proved (Figure 10). The first interesting observation was a difference in the attenuation of fibrosis capabilities in males, when animals were left to self-heal, to an extent different in respect to females (Figure 9). Confirmed also by investigation of collagens modulations (Figure 12-13), this difference was not due to a diverse metabolic activation of the toxicant (Figure 11). Liver fibrosis is a chronic disease, associated with many collateral diseases including reproductive dysfunction [Bubnov *et al*., 2017]. Circulating sexual hormones in our model of damage were measured (Figure 29) and interestingly a loss of significance in estradiol concentrations between females and males with a chronic hepatic damage was observed. This evidence reminded us an old paper by Furlong and collaborators (Furlong *et al*., 1949) and led us to speculate that this loss of significance could be associated with an increase in the urinary excretion of estradiol in females, due to an alteration in renal vasculature. This issue is an aspect which deserves to be evaluated in future studies. In parallel, other possible explanations for the decrease in serum estradiol levels in females which need to be investigated rely on a possible hormonal block following the inflammation and the stress induced by toxin used for chronic hepatic damage induction. Also these aspects are going to be explored in the next future.

An aspect which was then considered during my PhD has been a deep characterization of the injured hepatic milieu. The attention focused on matrix remodelling. The matrix dynamics analysis revealed an unexpected difference in MMP9 activity between males and females, associated with an accumulation of TIMP-1 in the parenchyma of injured females (Figures 14-15), while in males the protein showed non-significant modulations even though a trend to decrease with the continuation of chronic hepatic damage was apparent (Figure 15). A possible explanation of why injured females, even if allowed to self-heal, do not succeed to properly regenerate, differently from damaged males, could rely on an alteration in the homeostasis of MMP-TIMP during the chronic insult. Noteworthy,

during the 8 weeks of CCl_4 suspension, TIMP-1 significantly decreased in treated females and this was paralleled by an up-regulation of MMP9 mRNA, which was significantly higher than in males at the same time point (Figure 17). Data of the literature confirm our observation, demonstrating that TIMP-1 overexpression hinders the clearance of fibrotic matrix leading to extensive accumulation of interstitial ECM [Yoshiji *et al.*, 2002]. Furthermore, MMP-9 may promote hepatic stellate cell apoptosis in the presence of low levels of TIMP-1 [Ramachandran *et al*., 2012]. Once activated, MMP-9 functions to induce rapid turnover primarily of collagen IV and V, for reparative processes. MMP-9 is produced by HSC, inflammatory cells [Han, 2006; Calabro *et al*., 2014] as well as it is expressed in injured hepatocytes. The late increase in MMP9 activity from week 2 to week 6 and the subsequent decrease from week 6 to week 12 observed in females along with the increase in the amount of Collagen IV observed during the self-healing could be suggestive of the impairment of MMP pathway. Interestingly, overexpression of MMP-9 has been associated with defective tissue healing, suggesting that high levels of activated MMP-9 lead to excessive degradation of extracellular matrix proteins [Choi *et al*., 2000].

Hepatocyte apoptosis was reported to be significantly reduced in the absence of MMP-9 after hepatic IRI [Hamada *et al*., 2009]. In our injury model, which mimics a completely different experimental setting, after 2 weeks of CCl_4 administration, in male was observed a significantly higher hepatocytes apoptosis in respect to females (Figure 16), concomitantly with the prominence of MMP9 activity (Figure 14). However, with the progression of the injury, even though in males the activity of MMP9 decreased, the amount of Asp-175$^+$ cells increased (Figure 16). The reduction of apoptotic cells observed during the self-healing (Figure 16) was accompanied only in males by a reduction in MMP9 activity, whilst in females in the same time frame the activity of MMP9 remained almost invariable (Figure 14).

MMP-9 together with MMP-12 were identified in a CD11b^{hi} F4/80^{int} Ly-6C^{lo} macrophage subset associated with resolution of fibrosis [Ramachandran *et al.*, 2012]. MMP-9 expression was detected in the early stages of hepatic fibrogenesis and it may release/activate TGF-β, a major pro-fibrotic cytokine, from ECM reservoirs [Knittel *et al*., 2000; Yu *et al.*, 2000]. In our model of chronic injury the transcript of MMP9 was found almost comparable between males and females with the exception of the recovery group in which the transcript was found upregulated in females. Moreover a gradual decrease of MMP9 mRNA was observed along the chronic injury (Figure 17). This paralleled with the progressive decrease of activated F4/80$^+$ macrophages observed solely in males, not in females (Figure 18). Of note, in the parenchyma of females an increase of F4/80$^+$ macrophages was demonstrated, with a concomitant increase in MMP9 mRNA (Figure 18 and Figure 17 respectively).

We could speculate that in this experimental setting, the F4/80$^+$ population is not directly associated with a restorative phenotype, at least in females.

MMP-9 is sensitive to cytokines and growth factors, however, and in response to their induction, there is an immediate and substantial increase in MMP-9 in affected tissues. In addition, inflammatory cells infiltrating the injured area release MMP-9 [Roach *et al*., 2002]. This is observed early in treated males, during the chronic liver damage development, when the higher MMP9 activity is associated with the higher percentage of F4/80$^+$ macrophages observed (Figure 14 and Figure 18, respectively). At one extreme, macrophages may be classically activated by Toll-like receptor ligands and pro-inflammatory mediators, including TNF-α, IL-1 and IFN-γ. In this early phase of the chronic damage, the serum immune profile of males showed higher levels of IL-6 (Th1 response), TNF-α (Th1 response), M-CSF, properly counterbalanced by high levels of IL-4 (Th2 response), while GM-CSF, IL-2 (Th1 response) and IL-17 (Th1 response) were lower in respect to females. Interestingly, control males exhibited higher basal levels of both GM-CSF and IL-2, if compared to control females (Figure 28 and data not shown). On the contrary, when considering the immune profile of injured males during the self-healing, it dramatically changed, being characterized by higher levels of IFN-γ, GM-CS, IL-12β and IL-2, in respect to females. Data from literature confirm a critical role for circulating IL-6 and TNF-α (high levels in early phases of the injury) during liver regeneration [Yamada *et al*., 1997; Streetz *et al*., 2000]. These literature data explain our observations on male milieu, which appeared more prone to resorb excess of matrix in respect to females.

The chronically-injured hepatic parenchyma was further characterized for both VEGFA and IL-6. The results of VEGFA mRNA modulations (Figure 21) unveiled significant differences in the amount of the transcript between females and males both at week 2 and 6. Interestingly, the upregulation of 100% of VEGFA mRNA observed in males at week 6 in respect to females is sustained by protein data at week 12 (Figure 20). When animals are left to self-heal, both VEGFA mRNA and protein increased, and this could be considered an index of revascularization and/or neo-angiogenesis, fundamental for an organ to regenerate. Moreover its role in angiocrine signalling is well recognized: it is demonstrated that VEGF is essential for CCl_4-induced liver fibrosis resolution through matrix metalloproteinase 13 and CXCL9 [Kostallari *et al*., 2016]. MMP-13 is an interstitial collagenase, highly specific protease capable of degrading insoluble fibrillary collagens, especially type I collagen, suggesting a role for MMP-13 in liver fibrogenesis, as an anti-fibrotic metalloproteinase. MMP-13 upregulation in the liver has been correlated with the change from normal to abnormal matrix turnover in the CCl_4 injury model [Calabro *et al*., 2014]. Moreover, MMP-13 gene deletion results in a retarded resolution of CCl_4-induced fibrosis [Fallowfield *et al*., 2007]. However, it has also been reported that MMP-13 mediates the initial inflammation and contributes to accelerate fibrogenesis in cholestatic

livers [Uchinami *et al*., 2006]. MMP13 is a macrophage-derived interstitial collagenase known to drive fibrosis resolution. Scar associated macrophages –SAMs- could be considered the major source for this MMP. An overall decrease of MMP13 mRNA from week 2 to the end of the self-healing both in males and females was observed in our model of hepatic damage (Figure 24), although at the end of the intoxication, its levels were significantly higher in males than in females. IL-12β represents a key driver of Th1 and Th17 responses and its contribution in inflammation and fibrosis has been demonstrated in a model of pulmonary fibrosis by Huaux and colleagues where a role in exacerbating the recruitment of macrophages was demonstrated. CXCL9 is recognized as an angiostatic and anti-fibrotic chemokine and a strong counter-regulatory molecule of VEGF-driven aberrant liver vascularization and perfusion in vitro and in vivo [Sahin *et al*., 2012]. CXCL9 mRNA was regulated in treated males across the chronic injury, differently from females, although it was found upregulated in females in respect to males both at week 2 and 12 of about 577% and 168%, respectively (Figure 26). IL-12β mRNAs modulations data (Figure 25), in particular the upregulation of the transcript in females in respect to males both at week 2 and after the period of self-recovery, are suggestive of a milieu more fibrosis- and inflammation-prone in the former in respect to the latter. Moreover, it could be speculated that, during the self-healing, a key event occurs which accounts for the decrease in males of both MMP13 and CXCL9 mRNAs along with the increase in VEGFA mRNA. It is noteworthy that something different occurs in females during the self-healing, despite the observed increase in VEGFA mRNA, since, as previously discussed, treated females presented with an up-regulation of CXCL9 mRNA if compared to males of about 168%, and interestingly of IL-12β of about 134%. The study of neoangiogenesis and if an abnormal angioarchitecture distinguishes the liver of treated males and females is ongoing as part of a distinct research work.

Figure 22 and 23 resume evidences on IL-6 protein and mRNA regulation in our experimental setting. From the literature we learned that IL-$6^{-/-}$ mice develop more severe liver fibrosis after chronic CCl_4 treatment or bile duct ligation, if compared to wild type mice, suggesting that IL-6 may exert a protective role in the liver also during the progression of chronic damage towards cirrhosis [Kovalovich *et al*., 2000; Tiberio *et al*., 2008]. Furthermore a role for IL-6 in hepatocytes apoptosis inhibition is recognized [Streetz *et al*., 2000]. IL-6 mRNA increased in treated males along the chronic damage, remaining almost constant in treated females (Figure 23), whilst the protein was most abundant in males than in females in the onset of chronic damage (Figure 22). We speculated that in the early phase of the injury, males are allowed to define a distinct and fibrinolysis-prone milieu, differently from females.

The next step was the characterization of the immune components infiltrating the injured hepatic parenchyma. As evidenced in Figure 27, the dendritic component was almost equally represented

between males and females, and it was inversely correlated with the severity of the injury. Also the component $CD11b^{+}Gr1^{low}$, associated with the hepatic monocytes/macrophages fraction infiltrating the liver from the circulation, which exhibits an anti-inflammatory and tissue protective phenotype, was found at comparable % in treated males and females at week 2 (males week 2 vs females week 2: 2.16±0.98 vs 1.93±0.6 p=0.852 data not shown). Interestingly KCs and $F4/80^{+}GATA6^{+}$ population clearly distinguished between males and females. As suggested by Figure 27, after the period of recovery, a residual population of KCs in females and of restorative macrophages in males, respectively, were apparent. Our hypothesis is that during the phase of self-healing, in females the presence of KCs, expressing CXCL9 and other inflammatory chemokines, as IL-12β, could represent the crucial event which impairs the ECM excess resorption, perturbing the physiological process of scar tissue remodelling. In this respect Ikeda and colleagues demonstrated that macrophages/KCs expressing CXCL9 play a critical role in AIH progression [Ikeda *et al*., 2014]. Of course, it is plausible that other cells capable of expressing MMPs and secreting chemokines may also contribute to regulation of matrix degradation by releasing collagenolytic enzymes into the pericellular milieu.
In conclusions, evidences of this PhD thesis highlight the presence in mice of gender differences both in the onset and resolution phases of chronic liver injury. These differences result closely interconnected to a distinct immune milieu which organizes after the injured organ is left to self-recover.

Appendix

During this PhD Thesis, I have been also involved in the following projects, two of which have already produced a publication, the third one being a submitted paper.

1. Analysis of sex-related differences associated with inflammatory responses following an acute hepatic damage induced by toxin. Molecular Real-Time PCR analysis for the analysis of major transcripts associated with macrophages flows was one of the activity developed by my-self, starting from stored liver specimens of animals acutely injured and treated or not with a chemical, namely flutamide, which is an antagonist of androgen receptor. Moreover the IHC study of hepatocytes proliferation, after the set-up of the technique. The animal model of acute injury, as well, was established and set-up by my-self.
The work produced the following publication, as co-first author. *Sex-dependent differences in inflammatory responses during liver regeneration in a murine model of acute liver injury*. Bizzaro D*****, **Crescenzi Marika*,** Di Liddo R, Arcidiacono D, Cappon A, Bertalot T, Amodio V, Tasso A, Stefani A, Bertazzo V, Germani G, Frasson C, Basso G, Parnigotto P, Alison MR, Burra P, Conconi MT, Russo FP. Clin Sci (Lond). 2018 Jan 25; 132(2):255-272. doi: 10.1042/CS20171260. *****equal contribution

2. Within a collaboration with the Department of Biomedical Science of the University of Padova, I developed a slightly different model (in respect to the one developed for this PhD Thesis work) of mice chronic hepatic damage, in order to precisely time the different stages of fibrosis development and ultimately, understanding the observations that our colleagues obtained in sera of humans with an hepatic disease with various grades of severity.
This fruitful collaboration resulted in the following publication, as second author. *Heparanase and macrophage interplay in the onset of liver fibrosis.* Secchi MF, **Crescenzi Marika**, Masola V, Russo FP, Floreani A, Onisto M. Sci Rep. 2017 Nov 2; 7(1):14956. doi: 10.1038/s41598-017-14946-0.

3. During the third PhD year, an interdisciplinary and stimulating collaboration with the group of Prof. Viola Antonella (Department of Biomedical Sciences of the University of Padova) involved me in the study in a completely different model of hepatic damage (a model of Primary Sclerosing Cholangitis –PSC-), namely an example of immune-mediated chronic biliary disorders, of the effects of human extracellular vesicles (hEVs) derived from MSCs *in vivo* from the point of view of liver damage and fibrogenesis. The results obtained with IHC experiments for $F4/80^{+}$ activated

macrophages and activated HSCs, considered in the entire study, unveil an important anti-fibrotic effect of MSC-derived hEVs in the pathogenesis of PSC in the MDR2$^{-/-}$ mouse model.

This collaboration produced the following publication, which is in this moment under review. *Administration of Extracellular Vesicles for the treatment of Primary Sclerosis Cholangitis: preclinical data in MDR2 knockout mice*. Roberta Angioni*, Bianca Calì*, Vasanthy Vigneswara, **Marika Crescenzi**, Martin Hoogduijn, Philip N Newsome, Maurizio Muraca, Francesco Paolo Russo, Antonella Viola. Gut. *Under revision*

References

Abu Rmilah A., Zhou W., Nelson E., Lin L., Amiot B., Nyberg S.L. Understanding the marvels behind liver regeneration. Wiley Interdiscip Rev Dev Biol. 2019, 8(3): e340. doi: 10.1002/wdev.340

Azuma H., Paulk N., Ranade A., Dorrell C., Al-Dhalimy M., Ellis E., Strom S., Kay M.A., Finegold M., Grompe M. Robust expansion of human hepatocytes in Fah(−/−)/Rag2(−/−)/Il2rg (−/−) mice. Nature Biotechnology 2007, 25(8): 903–910. doi: 10.1038/nbt1326

Bataller R. and Brenner D.A. Liver fibrosis. Journal of Clinical Investigation 2005, 115(2): 209–218. doi: 10.1172/JCI200524282

Bedossa P., Paradis V. Liver extracellular matrix in health and disease. J Pathol 2003, 200: 504– 515. doi: 10.1002/path.1397

Bilzer M., Roggel F., Gerbes A.L. Role of Kupffer cells in host defense and liver disease. Liver Int. 2006, 26: 1175–1186. doi 10.1111/j.1478-3231.2006.01342.x

Bishayee A. The role of inflammation and liver cancer. Adv Exp Med Biol 2014, 816: 401–435. doi: 10.1007/978-3-0348-0837-8_16

Bonnans C., Chou J., Werb Z. Remodelling the extracellular matrix in development and disease. Nat Rev Mol Cell Biol 2014, 15: 786–801. doi: 10.1038/nrm3904

Boulter L., Govaere O., Bird T.G., Radulescu S., Ramachandran P., Pellicoro A., Ridgway R.A., Seo S.S., Spee B., Van Rooijen N., Sansom O.J., Iredale J.P., Lowell S., Roskams T., Forbes S.J. Macrophage-derived Wnt opposes Notch signaling to specify hepatic progenitor cell fate in chronic liver disease. Nat Med 2012, 18: 572-9. doi: 10.1038/nm.2667

Chen G.Y., Nunez G. Sterile inflammation: Sensing and reacting to damage. Nat Rev Immunol 2010, 10: 826–837. doi: 10.1016/j.jaut.2009.08.008

Cordero-Espinoza L., Huch M. The balancing act of the liver: tissue regeneration versus fibrosis. J Clin Invest 2018, 128(1): 85-96. doi: 10.1172/JCI93562

Cox A.G. and Goessling W. The lure of zebrafish in liver research: regulation of hepatic growth in development and regeneration. Curr Opin Genet Dev 2015, 32: 153-161. doi: 10.1016/j.gde.2015.03.002

Desai S.S., Tung J.C., Zhou V.X., Grenert J.P., Malato Y., Rezvani M., Español-Suñer R., Willenbring H., Weaver V.M., Chang T.T. Physiological ranges of matrix rigidity modulate primary mouse hepatocyte function in part through hepatocyte nuclear factor 4 alpha. Hepatology 2016, 64: 261–275. doi: 10.1002/hep.28450

Desmet V.J., Roskams T. Cirrhosis reversal: a duel between dogma and myth. J Hepatol 2004, 40(5): 860–867. doi: 10.1016/j.jhep.2004.03.007

Duarte S., Baber J., Fujii T., Coito A.J. Matrix metalloproteinases in liver injury, repair and fibrosis. Matrix Biology 2015, 44-46: 147–156. doi: 10.1016/j.matbio.2015.01.004

Duffield J.S., Forbes S.J, Constandinou C.M., Clay S., Partolina M., Vuthoori S., Wu S., Lang R., Iredale J.P. Selective depletion of macrophages reveals distinct, opposing roles during liver injury and repair. Journal of Clinical Investigation 2005, 115(1): 56–65. doi: 10.1172/JCI22675

Fanjul-Fernandez M., Folgueras A.R., Cabrera S., Lopez-Otin C. Matrix metalloproteinases: evolution, gene regulation and functional analysis in mouse models. Biochim Biophys Acta 2010, 1803: 3–19. doi: 10.1016/j.bbamcr.2009.07.004

Fausto N., Campbell J.S., Riehle K.J. Liver regeneration. Hepatology 2006, 43(2 Suppl 1): S45–S53. doi: 10.1002/hep.20969

Fava G., Glaser S., Francis H., Alpini G. The immunophysiology of biliary epithelium. Semin Liver Dis 2005, 25:251–264. doi: 10.1055/s-2005-916318

Fielding C.A., Jones G.W., McLoughlin R.M., McLeod L., Hammond V.J., Uceda J., Williams A.S., Lambie M., Foster T.L., Liao C.T., Rice C.M., Greenhill C.J., Colmont C.S., Hams E., Coles B., Kift-Morgan A., Newton Z., Craig K.J., Williams J.D., Williams G.T., Davies S.J., Humphreys I.R., O'Donnell V.B., Taylor P.R., Jenkins B.J., Topley N., Jones S.A. Interleukin-6 signaling drives

fibrosis in unresolved inflammation. Immunity 2014, 40(1): 40–50. doi: 10.1016/j.immuni.2013.10.022

Forbes S.J. and Newsome P.N. Liver regeneration -mechanisms and models to clinical application. Nature Reviews Gastroenterology and Hepatology 2016, 13(8): 473–485. doi: 10.1038/nrgastro.2016.97

Friedman S.L. Hepatic stellate cells: protean, multifunctional, and enigmatic cells of the liver. Physiological Reviews 2008, 88(1): 125–172. doi: 10.1152/physrev.00013.2007

Furlong E., Krichesky E., Glass S.J. Effect of carbon tetrachloride-feeding on estrogen escretion in the normal female guinea pig. Endocrinology 1949, 45(1): 1-9. doi: 10.1210/endo-45-1-1

Gabbia D., Pozza A.D., Albertoni L., Lazzari R., Zigiotto G., Carrara M., Baldo V., Baldovin T., Floreani A., De Martin S. Pregnane X receptor and constitutive androstane receptor modulate differently CYP3A-mediated metabolism in early- and late-stage cholestasis. World J Gastroenterol 2017, 23(42): 7519-7530. doi: 10.3748/wjg.v23.i42.7519

Gao B., Jeong W.I., Tian Z. Liver: An organ with predominant innate immunity. Hepatology 2008, 47: 729–736. doi: 10.1002/hep.22034

Gieling R.G., Wallace K., and Han Y.P. Interleukin-1 participates in the progression from liver injury to fibrosis. American Journal of Physiology-Gastrointestinal and Liver Physiology 2009, 296(6): G1324–G1331. doi: 10.1152/ajpgi.90564.2008

Gilliver S.C., Ruckshanthi J.P., Hardman M.J., Nakayama T. and Ashcroft G.S. Sex dimorphism in wound healing: the roles of sex steroids and macrophage migration inhibitory factor. Endocrinology 2008, 149: 5747–5757. doi: 10.1210/en.2008-0355

Goessling W., North T.E., Lord A.M., Ceol C., Lee S., Weidinger G., Bourque C., Strijbosch R., Haramis A.P., Puder M., Clevers H., Moon R.T., Zon L.I. APC mutant zebrafish uncover a changing temporal requirement for wnt signaling in liver development. Dev Biol 2008, 320: 161-74. doi: 10.1016/j.ydbio.2008.05.526

Guicciardi M.E., Malhi H., Mott J.L., Gores G.J. Apoptosis and necrosis in the liver. Comprehensive Physiology, vol. 3, no. 2, 2013. doi: 10.1002/cphy.c120020

Hammerich L., Bangen J.M., Govaere O., Zimmermann H.W., Gassler N., Huss S., Liedtke C., Prinz I., Lira S.A., Luedde T., Roskams T., Trautwein C., Heymann F., Tacke F. Chemokine receptor CCR6-dependent accumulation of γδ T cells in injured liver restricts hepatic inflammation and fibrosis. Hepatology 2014, 59(2): 630–642. doi: 10.1002/hep.26697

He J., Lu H., Zou Q. and Luo L. Regeneration of liver after extreme hepatocyte loss occurs mainly via biliary transdifferentiation in zebrafish. Gastroenterology 2014, 146: 789-800 e8. doi: 10.1053/j.gastro.2013.11.045

Henderson N.C. and Iredale J.P. Liver fibrosis: cellular mechanisms of progression and resolution. Clinical Science 2007, 112(5): 265–280. doi: 10.1042/CS20060242

Heymann F., Hamesch K., Weiskirchen R. and Tacke, F. The concanavalin A model of acute hepatitis in mice. Lab. Anim. 2015, 49: 12–20. doi: 10.1177/0023677215572841

Higgins G.M. and Anderson R.M. Experimental pathology of the liver: restoration of the liver of the white rat following partial surgical removal. Archives of Pathology 1931, 12: 186–202.

Holt M.P., Cheng L., Ju C. Identification and characterization of infiltrating macrophages in acetaminophen induced liver injury. Journal of Leukocyte Biology 2008, 84(6): 1410–1421. doi: 10.1189/jlb.0308173

Huang M., Chang A., Choi M., Zhou D., Anania F.A., Shin C.H. Antagonistic interaction between Wnt and Notch activity modulates the regenerative capacity of a zebrafish fibrotic liver model. Hepatology 2014, 60: 1753-66. doi: 10.1002/hep.27285

Iimuro Y., Nishio T., Morimoto T., Nitta T., Stefanovic B., Choi S.K., Brenner D.A., Yamaoka Y. Delivery of matrix metalloproteinase-1 attenuates established liver fibrosis in the rat. Gastroenterology 2003, 124(2): 445–458. doi: 10.1053/gast.2003.50063

Jiang F., Chen J., Ma X., Huang C., Zhu S., Wang F., Li L., Luo L., Ruan H., Huang H. Analysis of mutants from a genetic screening reveals the control of intestine and liver development by many common genes in zebrafish. Biochem Biophys Res Commun 2015, 460: 838-44. doi: 10.1016/j.bbrc.2015.03.119

Jiao J., Sastre D., Fiel M.I., Lee U.E., Ghiassi-Nejad Z., Ginhoux F., Vivier E., Friedman S.L., Merad M., Aloman C. Dendritic cell regulation of carbon tetrachloride-induced murine liver fibrosis regression. Hepatology 2012, 55(1): 244–255. doi: 10.1002/hep.24621

Karlmark K.R., Weiskirchen R., Zimmermann H.W., Gassler N., Ginhoux F., Weber C., Merad M., Luedde T., Trautwein C., Tacke F. Hepatic recruitment of the inflammatory $Gr1^{+}$ monocyte subset upon liver injury promotes hepatic fibrosis. Hepatology 2009, 50(1): 261–274. doi: 10.1002/hep.22950

Knolle P., Schlaak J., Uhrig A., Kempf P., Meyer zum Buschenfelde K.H., Gerken, G. Human Kupffer cells secrete IL-10 in response to lipopolysaccharide (LPS) challenge. J Hepatol 1995, 22: 226–229. doi: 10.1016/0168-8278(95)80433-1

Kolios G., Valatas V., and Kouroumalis E. Role of Kupffer cells in the pathogenesis of liver disease. World Journal of Gastroenterology 2006, 12(46): 7413–7420. doi: 10.3748/wjg.v12.i46.7413

Krämer B., Körner C., Kebschull M., Glässner A., Eisenhardt M., Nischalke H.D., Alexander M., Sauerbruch T., Spengler U., Nattermann J. Natural killer $p46^{high}$ expression defines a natural killer cell subset that is potentially involved in control of hepatitis C virus replication and modulation of liver fibrosis. Hepatology 2012, 56(4): 1201–1213. doi: 10.1002/hep.25804

Lachowski D., Cortes E., Rice A., Pinato D., Rombouts K., Del Rio Hernandez A. Matrix stiffness modulates the activity of MMP-9 and TIMP-1 in hepatic stellate cells to perpetuate fibrosis. Sci Rep 2019, 9(1): 7299. doi: 10.1038/s41598-019-43759-6

Li F., Huang Q., Chen J., Peng Y., Roop D.R., Bedford J.S., Li C.Y. Apoptotic cells activate the "phoenix rising" pathway to promote wound healing and tissue regeneration. Sci Signal 2010, 3:ra13. doi: 10.1126/scisignal.2000634

Li H, You H., Fan X., and Jia J. Hepatic macrophages in liver fibrosis: pathogenesis and potential therapeutic targets. BMJ Open Gastroenterology 2016, 3(1): e000079. doi: 10.1136/bmjgast-2016-000079

Mantovani A., Sica A., Locati M. Macrophage polarization comes of age. Immunity 2005, 23(4): 344–346. doi: 10.1016/j.immuni.2005.10.001

Mao S.A., Glorioso J.M., Nyberg S.L. Liver regeneration. Translational Research 2014, 163(4): 352–362. doi: 10.1016/j.trsl.2014.01.005

Medzhitov R. Origin and physiological roles of inflammation. Nature 2008, 454: 428–435. doi: 10.1038/nature07201

Michalopoulos G.K. Liver regeneration. Journal of Cellular Physiology 2007, 213(2): 286–300. doi: 10.1002/jcp.21172

Mittal D., Gubin M.M., Schreiber R.D., Smyth M.J. New insights into cancer immunoediting and its three component phases–elimination, equilibrium and escape. Curr Opin Immunol 2014, 27: 16–25. doi: 10.1016/j.coi.2014.01.004

Nelson D.R., Lauwers G.Y., Lau J.Y.N., Davis G.L. Interleukin 10 treatment reduces fibrosis in patients with chronic hepatitis C: a pilot trial of interferon nonresponders. Gastroenterology 2000, 118(4): 655–660. doi: 10.1016/s0016-5085(00)70134-x

Novo E., Cannito S., Morello E., Paternostro C., Bocca C., Miglietta A., Parola M. Hepatic myofibroblasts and fibrogenic progression of chronic liver diseases. Histology and Histopathology 2015, 30(9): 1011–1032. doi: 10.14670/HH-11-623

Palmes D. and Spiegel H.U. Animal models of liver regeneration. Biomaterials 2004, 25(9): 1601–1611. doi: 10.1016/s0142-9612(03)00508-8

Piñeiro Fernández J., Luddy K.A., Harmon C., O'Farrelly C. Hepatic Tumor Microenvironments and Effects on NK Cell Phenotype and Function. Int J Mol Sci 2019, 20: 4131. doi:10.3390/ijms20174131

Pritchard M.T. and Apte U. Models to study liver regeneration In Apte U (Ed.), Liver regeneration: Basic mechanisms, relevant models and clinical applications. Cambridge, MA: Academic press 2015, 15–40

Protzer U., Maini M.K., Knolle P.A. Living in the liver: Hepatic infections. Nat Rev Immunol 2012, 12: 201–213. doi: 10.1038/nri3169

Puche, J.E., Saiman Y., Friedman S.L., Hepatic stellate cells and liver fibrosis. Compr Physiol 2013, 3(4): 1473-92. doi: 10.1002/cphy.c120035

Radaeva S., Sun R., Jaruga B., Nguyen V.T., Tian Z., Gao B. Natural killer cells ameliorate liver fibrosis by killing activated stellate cells in NKG2Ddependent and tumor necrosis factor-related apoptosis-inducing ligand-dependent manners. Gastroenterology 2006, 130(2): 435–452. doi: 10.1053/j.gastro.2005.10.055

Ramachandran P., Iredale J.P. Liver fibrosis: a bidirectional model of fibrogenesis and resolution. QJM 2012, 105(9): 813–817. a. doi: 10.1093/qjmed/hcs069

Ramadori G., Armbrust T. Cytokines in the liver. Eur J Gastroenterol Hepatol 2001, 13: 777–784. doi: 10.1097/00042737-200107000-00004

Ramachandran P., Pellicoro A., Vernon M.A., Boulter L., Aucott R.L., Ali A., Hartland S.N., Snowdon V.K., Cappon A., Gordon-Walker T.T., Williams M.J., Dunbar D.R., Manning J.R., van Rooijen N., Fallowfield J.A., Forbes S.J., Iredale J.P. Differential Ly-6C expression identifies the recruited macrophage phenotype, which orchestrates the regression of murine liver fibrosis. Proc Natl Acad Sci U S A. 2012, 109(46): E3186–E3195. b. doi: 10.1073/pnas.1119964109

Sadler K.C., Krahn K.N., Gaur N.A. and Ukomadu C. Liver growth in the embryo and during liver regeneration in zebrafish requires the cell cycle regulator, uhrf1. Proc Natl Acad Sci U S A 2007, 104: 1570-5. doi: 10.1073/pnas.0610774104

Saile B., Matthes N., Knittel T., Ramadori G. Transforming growth factor beta and tumor necrosis factor alpha inhibit both apoptosis and proliferation of activated rat hepatic stellate cells. Hepatology 1999, 30(1): 196–202. doi: 10.1002/hep.510300144

Saito M., Iwawaki T., Taya C., Yonekawa H., Noda M., Inui Y., Mekada E., Kimata Y., Tsuru A., Kohno K. Diphtheria toxin receptor mediated conditional and targeted cell ablation in transgenic mice. Nat Biotechnol 2001, 19: 746–750. doi: 10.1038/90795

Santodomingo-Garzon T., Swain M.G. Role of NKT cells in autoimmune liver disease. Autoimmun Rev 2011, 10: 793–800. doi: 10.1016/j.autrev.2011.06.003

Schwinge D., Carambia A., Quaas A., Krech T, Wegscheid C, Tiegs G, Prinz I, Lohse AW, Herkel J, Schramm C. Testosterone suppresses hepatic inflammation by the downregulation of IL-17, CXCL-9, and CXCL-10 in a mouse model of experimental acute cholangitis. J Immunol 2015, 194: 2522–2530. doi: 10.4049/jimmunol.1400076

Seki S., Nakashima H., Nakashima M., Kinoshita M. Antitumor immunity produced by the liver Kupffer cells, NK cells, NKT cells, and CD8 CD122 T cells. Clin Dev Immunol 2011, 2011: 868345. doi: 10.1155/2011/868345

Seki E., Schwabe R.F. Hepatic inflammation and fibrosis: Functional links and key pathways. Hepatology 2015, 61: 1066–1079 65. doi: 10.1002/hep.27332

Shapouri-Moghaddam A., Mohammadian S., Vazini H., Taghadosi M., Esmaeili S.A., Mardani F., Seifi B., Mohammadi A., Afshari J.T., Sahebkar A. Macrophage plasticity, polarization, and function in health and disease. Journal of Cellular Physiology 2018, 233(9): 6425–6440. doi: 10.1002/jcp.26429

Sica A., Invernizzi P., Mantovani A. Macrophage plasticity and polarization in liver homeostasis and pathology. Hepatology 2014, 59: 2034–2042. doi: 10.1002/hep.27332

Stout R. D., Suttles J. Functional plasticity of macrophages: reversible adaptation to changing microenvironments. Journal of Leukocyte Biology 2004, 76(3): 509–513. doi: 10.1189/jlb.0504272

Sudo K., Yamada Y., Saito K., Shimizu S., Ohashi H., Kato T., Moriwaki H., Ito H., Seishima M. TNF-alpha and IL-6 signals from the bone marrow derived cells are necessary for normal murine liver regeneration. Biochim. Biophys. Acta 2008, 1782: 671–679. doi: 10.1016/j.bbadis.2008.09.010

Tacke F. and Zimmermann H.W. Macrophage heterogeneity in liver injury and fibrosis. Journal of Hepatology 2014, 60(5): 1090–1096. doi: 10.1016/j.jhep.2013.12.025

Thomas J.A., Pope C., Wojtacha D., Robson A.J., Gordon-Walker T.T., Hartland S., Ramachandran P., Van Deemter M., Hume D.A., Iredale J.P., Forbes S.J. Macrophage therapy for murine liver fibrosis recruits host effector cells improving fibrosis, regeneration, and function. Hepatology 2011, 53 (6): 2003–2015. doi: 10.1002/hep.24315

Tiegs G., Lohse A.W. Immune tolerance: What is unique about the liver. J Autoimmun 2010, 34: 1–6. doi: 10.1016/j.jaut.2009.08.008

Tilg H., Kaser A., Moschen A.R. How to modulate inflammatory cytokines in liver diseases. Liver International 2006, 26(9): 1029–1039. doi: 10.1111/j.1478-3231.2006.01339.x

Tsutsui H., Nishiguchi S. Importance of Kupffer cells in the development of acute liver injuries in mice. Int J Mol Sci 2014, 15: 7711–7730. doi: 10.3390/ijms15057711

Tsutsui H., Cai X., and Hayashi S. Interleukin-1 family cytokines in liver diseases. Mediators of Inflammation 2015, 2015: 630265. doi: 10.1155/2015/630265

Ueda T., Shimada E., Urakawa T. Serum levels of cytokines in patients with colorectal cancer: Possible involvement of interleukin-6 and interleukin-8 in hematogenous metastasis. J Gastroenterol 1994, 29: 423–429

Vempati P., Karagiannis E.D., Popel A.S. A biochemical model of matrix metalloproteinase 9 activation and inhibition. J Biol Chem 2007, 282: 37585–37596. doi: 10.1074/jbc.M611500200

Verfaillie, C.M. Biliary cells to the rescue of Prometheus. Gastroenterology 2014, 146: 611-4. doi: 10.1053/j.gastro.2014.01.039

Vliegenthart A.D., Tucker C.S., Del Pozo J. and Dear J.W. Zebrafish as model organisms for studying drug-induced liver injury. Br J Clin Pharmacol 2014, 78: 1217-27. doi: 10.1111/bcp.12408

Wells R.G. Tissue mechanics and fibrosis. Biochim Biophys Acta 2013, 1832: 884–890. doi: 10.1016/j.bbadis.2013.02.007

Winau F., Hegasy G., Weiskirchen R., Weber S., Cassan C., Sieling P.A., Modlin R.L., Liblau R.S., Gressner A.M., Kaufmann S.H. Ito cells are liver-resident antigen-presenting cells for activating T cell responses. Immunity 2007, 26: 117–129. doi 10.1016/j.immuni.2006.11.011

Yang Y.M. and Seki E. TNFα in liver fibrosis. Current Pathobiology Reports 2015, 3(4): 253–261. doi: 10.1007/s40139-015-0093-z

Yu L.X., Ling Y., Wang H.Y. Role of nonresolving inflammation in hepatocellular carcinoma development and progression. NPJ Precis Oncol 2018, 2(1):6. eCollection 2018. doi: 10.1038/s41698-018-0048-z

Zimmermann H.W., Seidler S., Nattermann J., Gassler N., Hellerbrand C., Zernecke A., Tischendorf J.J., Luedde T., Weiskirchen R., Trautwein C., Tacke F. Functional contribution of elevated circulating and hepatic non-classical CD14+ CD16+ monocytes to inflammation and human liver fibrosis. PLoS One 2010, 5(6): article e11049. doi: 10.1371/journal.pone.0011049

Publications

1. *Sex-dependent differences in inflammatory responses during liver regeneration in a murine model of acute liver injury*. Bizzaro D*****, **Crescenzi M*,** Di Liddo R, Arcidiacono D, Cappon A, Bertalot T, Amodio V, Tasso A, Stefani A, Bertazzo V, Germani G, Frasson C, Basso G, Parnigotto P, Alison MR, Burra P, Conconi MT, Russo FP. Clin Sci (Lond). 2018 Jan 25; 132(2):255-272. doi: 10.1042/CS20171260. *** equal contribution**

2. *Heparanase and macrophage interplay in the onset of liver fibrosis*. Secchi MF, **Crescenzi M**, Masola V, Russo FP, Floreani A, Onisto M. Sci Rep. 2017 Nov 2; 7(1):14956. doi: 10.1038/s41598-017-14946-0.

3. *Administration of Extracellular Vesicles for the treatment of Primary Sclerosis Cholangitis: preclinical data in MDR2 knockout mice*. Roberta Angioni*, Bianca Calì*, Vasanthy Vigneswara, **Marika Crescenzi**, Martin Hoogduijn, Philip N Newsome, Maurizio Muraca, Francesco Paolo Russo, Antonella Viola. Journal of Extracellular Vesicles, *Manuscript submitted*

4. *Inside the dimorphism in fibrosis development and regression in a murine model of chronic hepatic damage*. **Marika Crescenzi**, Chiara Frasson, Annalisa Stefani, Marina Bortolami, Laura Astolfi, Valentina Bertazzo, Sara De Martin, Daniela Gabbia, Maria Teresa Conconi, Patrizia Burra, Francesco Paolo Russo. *Manuscript in preparation*